A secretagogin locus of the mammalian hypothalamus controls stress hormone release

Running title: Secretagogin regulates CRH release

Roman Romanov[1,2,*], Alan Alpar[1,*,$,#], Ming-Dong Zhang[1,2], Amit Zeisel[1], André Calas[3], Marc Landry[3], Matthew Fuszard[4], Sally L. Shirran[4], Robert Schnell[1], Arpad Dobolyi[5], Mark Olah[6], Lauren Spence[7], Jan Mulder[2,8], Henrik Martens[9], Miklos Palkovits[10], Mathias Uhlen[11], Harald H. Sitte[12], Catherine H. Botting[4], Ludwig Wagner[13], Sten Linnarsson[1], Tomas Hökfelt[2,++] & Tibor Harkany[1,14,++,#]

[1]Department of Medical Biochemistry & Biophysics, Karolinska Institutet, SE-17177 Stockholm, Sweden; [2]Department of Neuroscience, Karolinska Institutet, SE-17177 Stockholm, Sweden; [3]Laboratory for Central Mechanisms of Pain Sensitization, Interdisciplinary Institute for Neuroscience, CNRS UMR 5297, Université Bordeaux 2, Bordeaux, France; [4]School of Chemistry, University of St. Andrews, St. Andrews KY16 9ST, United Kingdom; [5]Department of Anatomy, Semmelweis University, H-1094 Budapest, Hungary; [6]Department of Human Morphology and Developmental Biology, Semmelweis University, H-1094 Budapest, Hungary; [7]Institute of Medical Sciences, University of Aberdeen, Aberdeen AB25 2ZD, United Kingdom; [8]Science for Life Laboratory, Karolinska Institutet, SE-17177 Stockholm, Sweden; [9]Synaptic Systems GmbH, D-37079 Göttingen, Germany; [10]Human Brain Tissue Bank and Laboratory, Semmelweis University, H-1094 Budapest, Hungary; [11]Science for Life Laboratory, Albanova University Center, Royal Institute of Technology, SE-10691 Stockholm, Sweden; [12]Center for Physiology and Pharmacology, Institute of Pharmacology, Medical University of Vienna, A-1090 Vienna, Austria; [13]University Clinic for Internal Medicine III, General Hospital Vienna, A-1090 Vienna, Austria and [14]Department of Molecular Neurosciences, Center for Brain Research, Medical University of Vienna, A-1090 Vienna, Austria.

*R.R. & A.A. contributed equally to this study. [++]T.Hö. & T.Ha. share senior authorship.

[$]Present address: Research Group of Experimental Neuroanatomy and Developmental Biology, Hungarian Academy of Sciences & Department of Anatomy, Semmelweis University, Budapest, Hungary

[#]*Address correspondence to:* **Tibor Harkany** (at the Karolinska Institutet); *Telephone*: +46 8 524 87656; *Fax*: +46 8 341 960; *e-mail*: Tibor.Harkany@ki.se or **Alan Alpar** (at the Semmelweis University); *e-mail:* alpar.alan@med.semmelweis-univ.hu

Author contributions

T.Ha. conceived the general idea of this study; R.R., A.A., M.-D.Z., H.H.S., S.L., T.Hö. and T.Ha. designed experiments; R.R., A.A., M.-D.Z., A.Z., M.L., M.F., S.L.S., R.S., A.D., M.O., L.S., M.P., A.C., C.H.B. performed experiments and analyzed data; J.M., H.M., M.U. and L.W. contributed unique reagents, R.R., A.A., T.Hö. and T.Ha. wrote the manuscript. *All Authors commented on the manuscript and approved its submission*.

Conflict of interest

The Authors declare that they have no competing financial interests.

Abstract

A hierarchical hormonal cascade along the hypothalamo-pituitary-adrenal axis orchestrates bodily responses to stress. Although corticotropin-releasing hormone (CRH), produced by parvocellular neurons of the hypothalamic paraventricular nucleus (PVN) and released into the portal circulation at the median eminence, is known to prime downstream hormone release, the molecular mechanism regulating phasic CRH release remains poorly understood. Here, we find a cohort of parvocellular cells interspersed with magnocellular PVN neurons expressing secretagogin. Single-cell transcriptome analysis combined with protein interactome profiling identifies secretagogin neurons as a distinct CRH-releasing neuron population reliant on secretagogin's Ca^{2+}-sensor properties and protein-interactions with the vesicular traffic and exocytosis release machineries to liberate this key hypothalamic releasing hormone. Pharmacological tools combined with RNA interference demonstrate that secretagogin's loss-of-function occludes adrenocorticotropic hormone release from the pituitary and lowers peripheral corticosterone levels in response to acute stress. Cumulatively, these data define a novel secretagogin neuronal locus and molecular axis underpinning stress responsiveness.

Key words: acute stress / Ca^{2+} sensor / HPA axis / vesicular release

Introduction

Stress is the body's reaction to environmental conditions or noxious challenges. Fast adaptive responses to stress are reliant on a hierarchical hormonal cascade that adjusts and adapts to metabolic processes at the periphery (Selye et al, 1949; Baxter et al, 1972) to maximize energy expenditure in order to avoid adverse environments (Sapolsky et al, 1986; Swanson, 1991; Korte, 2001; de Kloet et al, 2005; McEwen, 2007). Stress hormone release is controlled by the hypothalamo-pituitary-adrenal (HPA) axis whose anatomical organization, allowing dynamic hormonal integration at the ligand and receptor levels and *via* extensive feedback and amplification loops, is well established (Kiss et al, 1984; Makino et al, 2002; Simmons et al, 2009; Tasker et al, 2011). In contrast, the localization and molecular identity of many neurosecretory neurons in rodents (particularly mouse) and humans are less well characterized, partly due to the rapid, phase-locked nature of the synthesis and release of stress hormones, limiting their usefulness as cellular markers (Swanson et al, 1989; Meister et al, 1990). In this context, the neuronal sites producing corticotropin-releasing hormone (CRH) (Spiess et al, 1981; Vale et al, 1981) in the paraventricular nucleus of the hypothalamus (PVN) (Swanson et al, 1986; Swanson et al, 1989; Herman et al, 1992; Sawchenko et al, 1993), as well as rate-limiting steps of CRH release into the hypophyseal portal circulation at the median eminence, are of particular significance since CRH liberates adrenocorticotropic hormone (ACTH) as the initial step of the peripheral stress response (Rivier et al, 1983; Kovacs et al, 1996). Nevertheless, detailed molecular underpinnings of CRH release remain to be defined.

The release of arginine-vasopressin (AVP) and oxytocin from magnocellular neurosecretory cells (Gainer et al, 2002), and of combinations of releasing and inhibitory hormones and other neuropeptides from parvocellular neurons (Swanson and Sawchenko, 1983) requires Ca^{2+}-dependent quantal exocytosis of dense core vesicles in response to afferent stimulation or direct metabolic challenges, entraining bursts of neuronal excitation in the PVN (Dutton et al, 1979; Cazalis et al, 1985; Carafoli et al, 2001; Petersen et al, 2005; Dayanithi et al, 2012). The priming of vesicular release is regulated by a multi-protein complex sequentially recruiting Ca^{2+} sensors, SNARE proteins and the docking machinery embedded in the presynaptic terminal (Sollner et al, 1993; Hata et al, 1993; Sutton et al, 1998; Pang et al, 2010). Ca^{2+} sensors are proteins that undergo conformational changes upon Ca^{2+} binding, sculpting inter-molecular interactions with downstream effectors to propagate action potential-dependent release events (Brose et al, 1992; Sudhof et al, 2009). As such, calbindin-D28k and calretinin were histochemically associated with magnocellular neurosecretory cells (Sanchez et al, 1992; Arai et al, 1993). In contrast, neuron-specific Ca^{2+} sensors were neither anatomically localized to nor functionally characterized in parvocellular hypothalamic neurons.

Recent neuroanatomical mapping places secretagogin, an EF-hand Ca^{2+}-binding protein (Wagner et al, 2000) into the PVN and adjacent pre-autonomic areas (Mulder et al, 2009; Maj et al, 2012). Despite the unexpected abundance of neurons expressing secretagogin mRNA and protein (secretagogin$^+$ neurons) in the mammalian hypothalamus, their phenotype, cumulatively defined by their fast neurotransmitter, neuropeptide and/or hormone contents, remains unknown. Moreover, and even if the proximity of secretagogin$^+$ neurons to the ventricular system along the longitudinal axis of the forebrain might indirectly infer a conserved role in secretory processes (Mulder et al, 2009), secretagogin's role in the nervous system remains elusive.

Here, we sought to address whether secretagogin marks a hitherto undescribed neurosecretory locus in the PVN. We have combined systems neuroanatomy, neurophysiology, single-cell transcriptomics and proteomics to unequivocally define secretagogin$^+$ neurons as a cohort of CRH-expressing parvocellular cells, partly interspersed within magnocellular domains of the PVN, and to show that this protein is a Ca^{2+} sensor modulating CRH release. By exploiting a genetic approach, we show that secretagogin-mediated CRH secretion is indispensable to prime ACTH release into the general circulation upon acute noxious stress (Makara et al, 1981). Cumulatively, our results define a key molecular mechanism gating the HPA axis upon stress-induced activation of CRH release from a molecularly distinct subtype of neuroendocrine parvocellular neurons in the hypothalamus.

Results

Secretagogin$^+$ neurons in the hypothalamic paraventricular nucleus

Recent neuroanatomical studies have identified abundant secretagogin expression in the hypothalamus (Mulder et al, 2009; Maj et al, 2012). Yet neither the detailed topology of secretagogin$^+$ neurons nor their functional significance in neuroendocrine control is known. Herein, we localized secretagogin$^+$ neurons, in descending order and along the longitudinal axis of the adult mouse brain, to paraventricular (PVN) > arcuate >> periventricular, dorsomedial and ventromedial hypothalamic nuclei (Fig. 1A-A_3,B). A dense secretagogin$^+$ cell group was found in the dorsolateral PVN, adjacent to and partly interspersed with magnocellular oxytocin$^+$ and AVP$^+$ magnocellular neurons, whose axons primarily descend into the posterior pituitary for the transient storage and "on-demand" release of these hormones (Bargmann, 1969; Gainer et al, 2002). Clearly, oxytocin, AVP and secretagogin segregated to non-overlapping cell cohorts (Fig. 1B,B_1). We extended this analysis to show that the supraoptic nucleus, an alternative site for oxytocin$^+$ and AVP$^+$ magnocellular neurons to reside (Swanson et al, 1983), lacked appreciable secretagogin expression (Fig. 1B_2). These data suggest that secretagogin$^+$ neurons belong to a discrete group of neurons interspersed with but not identical to oxytocin$^+$ or AVP$^+$ magnocellular neurons.

Next, we employed quantitative morphometry of secretagogin$^+$ neurons to cytoarchitecturally distinguish them from their oxytocin$^+$ or AVP$^+$ counterparts. Secretagogin$^+$ somata were significantly ($p < 0.05$) smaller in diameter than (Fig. 1B_3), but equality round (Fig. 1B_4) as those of either oxytocin$^+$ or AVP$^+$ neurons, suggesting parvocellular identity (Swanson et al, 1983). Nevertheless, secretagogin$^+$ axons occasionally terminated around blood vessels in the posterior pituitary and formed Herring body-like specializations that at points contained moderate levels of oxytocin (Fig. 1C-D_3). Cumulatively, these data suggest that secretagogin is broadly expressed in the PVN in a molecularly distinct neuronal contingent. Here, we focused on deciphering the identity and function of small-diameter "parvocellular-like" PVN neurons.

Secretagogin typifies a novel subclass of parvocellular neurons in the PVN

Protein localization at the subcellular level is a reliable predictor of protein function. Our high-resolution laser-scanning analysis (Fig. 1B,B_1) suggested that secretagogin, a predicted cytosolic protein (Birkenkamp-Demtroder et al, 2005), might be distributed ubiquitously, including dendrites and axons. We confirmed this notion at the ultrastructural level by pre-embedding immunoelectron microscopy (Fig. 2A-C). In the PVN, silver-intensified immunogold particles, revealing secretagogin's localization, were detected in the cytoplasm (Fig. 2A), particularly in submembranous compartments or in likely contact with the plasmalemma (Fig. 2A_1), and along the endoplasmic reticulum (Fig. 2A_2). Likewise, secretagogin was localized to dendrite shafts, often along their inner membrane surface (Fig. 2B). Moreover, we demonstrated secretagogin immunoreactivity in close proximity to the plasmalemma in nerve endings and possibly to dense core vesicles (Fig. 2C). Quantitative analysis of gold-intensified

silver particles in the PVN (somata, dendrtites) and the median eminence (axonal nerve endings) demonstrated that the majority of secretagogin associates to (endo-)membranes in neurons (that is, a given particle was <50 nm from the nearest membrane surface; Fig. 2D). Nevertheless, we found an opposite configuration in secretagogin distribution when comparing particle numbers on the plasmalemma and in the cytosol in neuronal somata and axons: in neuronal somata, the majority of secretagogin labeling appeared intracellular (Fig. 2D). In contrast, secretagogin localization along the plasma membrane outweighed cytosolic secretagogin content. These data suggest that secretagogin might play a role in controlling hormone or neuropeptide release.

Next, we have taken a neurophysiological approach to gain insights in the biophysical properties of secretagogin$^+$ neurons, and distinguish these from magnocellular, parvocellular or pre-autonomic PVN neurons using their properties to generate action potentials (APs), as well as 16 additional parameters (Table S1) as classification criteria (Luther et al, 2000; Luther et al, 2002). In rat, magnocellular neurons are characterized by a delay in generating the first AP upon current stimulation after pre-hyperpolarization (type I) due to a relatively high amplitude of their A-type currents (Luther et al, 2000; Lee et al, 2012). In contrast, AP delay is atypical for parvocellular neurons (type II) (Luther et al, 2000; Lee et al, 2012). Pre-autonomic neurons generate low threshold spikes and bursts given the activity of voltage-gated T-type Ca^{2+} channels (Stern, 2001; Lee et al, 2008). In whole-cell patch clamp experiments using *ex vivo* hypothalamus slice preparations we have analyzed >75 neurons in the PVN and pre-autonomic areas of juvenile mice (postnatal days 21-28). Using unified current- and voltage-clamp protocols, we designed novel classification criteria for mouse PVN neurons (Fig. 3), distinguishing 3 primary neuron types, which could then be clustered into 6 subtypes (Fig. 3E). In particular, type I neurons were reminiscent of magnocellular neurons from rat, including delayed AP generation after pre-hyperpolarization and high-amplitude A-type-like currents (Fig. 3A-A_3,D). This neuron population could be divided into *Ia* and *Ib* subgroups, based on outward current properties in recording conditions inactivating A-type channels (Fig. S1). *Ia* neurons generated outward currents typical for slowly-activated delayed-rectifying K^+ channels (Fig. 3D, Fig. S1). Meanwhile, *Ib* neurons exhibited transient, fast-activated currents upon depolarization (from -40 mV; Fig. S1). *Post-hoc* immunohistochemistry defined biocytin-filled magnocellular neurons as exclusively belonging to the *Ia* group.

Neurons that had histochemically been identified as secretagogin-positive (Fig. 3B-B_2) primarily belonged to type II mouse *parvocellular* neurons, and were equivalent in biophysical properties to those described in rat (Lee et al, 2012) or mouse (Wamsteeker Cusulin et al, 2013). Using the classification criteria introduced for type I neurons above, the type II cohort was subdivided as *IIa* and *IIb* neurons (Fig. S1). Nevertheless, we also identified some secretagogin$^+$ neurons with AP signatures similar but not identical to magnocellular cells (Fig. 3D,E), reinforcing our hypothesis on immunohistochemically undetectable AVP and/or oxytocin levels and introducing a novel scale of molecular heterogeneity amongst magnocellular PVN neurons.

Lastly, type III neurons were secretagogin-negative($^-$), low-threshold, and produced spike bursts upon somatic current injections (Fig. S1). These pre-autonomic cells, likewise sub-clustered as *IIIa* and *IIIb* (Fig. 3E), therefore were excluded as being secretagogin$^+$ neurons. Overall, these data suggest that the majority of secretagogin$^+$ neurons in the cluster as parvocellular cells in the PVN.

Secretagogin$^+$ parvocellular neurons express CRH

Parvocellular neurons in the PVN and other hypothalamic areas are diverse as to their neurochemical phenotypes (Swanson et al, 1983; Swanson et al, 1986; Everitt et al, 1986), with their majority producing releasing- or release-inhibiting hormones (Schally, 1978; Guillemin, 1978) that regulate trophormone secretion in the anterior pituitary via the *rete mirabile* of the hypothalamo-hypophyseal portal system, a concept originally described by (Harris, 1972). Considering that somatic neuropeptide and hormone detection is exceedingly difficult and relies on the permanent blockade of the anterograde axonal transport machinery (Cortes et al, 1990), we applied unbiased clustering analysis to single-cell transcriptome data (Tsafrir et al, 2005; Islam et al, 2014) generated from 130 cells dissociated from the mouse PVN. Overall, oxytocin, AVP, somatostatin, GABA and glutamate neurons exhibited discrete mRNA profiles in the PVN ("hot spots" in Fig. 4A,A$_1$; Table S3). In contrast, secretagogin$^+$ neurons, as well as CRH$^+$ and thyrotropin-releasing hormone (TRH)$^+$ neurons did not form separate clusters.

Next, we focused on which RNAs for hormones, neuropeptides and/or low-molecular weight neurotransmitters were present in secretagogin$^+$ neurons. We demonstrated the transcriptome-identity of these neurons by analyzing the absolute number of mRNA transcripts from 151 cells dispersed from the mouse PVN (Fig. 4A,A$_1$). We first tested the abundance of AVP, oxytocin, CRH and TRH gene transcripts (Fig. 4A,A$_1$), and show their broad variations, with particular reference to AVP and oxytocin mRNAs (that is, variations at 3-4 orders of magnitude; Fig. S2A). We defined a GABAergic hypothalamic contingent of ~30%, expressing Gad1 and/or Gad2 encoding respective glutamic acid decarboxylase 65 and 67 kDa (GAD65/GAD67) isoforms, as well as the vesicular GABA transporter (Slc32A1; Fig. 4A). Tyrosine hydroxylase and vesicular glutamate transporter 2 mRNAs were present in ~15% and ~10 % of the threshold-adjusted sample, respectively.

We then restricted our analysis of baseline mRNA expression values for each gene by ranking from minimum to maximum expression values (Fig. S2A) to increase homogeneity (Fig. 4A$_1$). As such, this cell population comprised 7.3% oxytocin$^+$ neurons (n = 11), 6.0% AVP$^+$ neurons (n = 9), 4.6% TRH$^+$ neurons (n = 7) and 6.6% CRH$^+$ neurons (n = 10). When dissecting the presence of gene transcripts of key pro-neuropeptides, our data from 151 cells revealed distinct somatostatin (n = 15 with high level), galanin (n = 11), cholecystokinin (n = 5), tachykinin 1 (n = 9), cocaine-and-amphetamine regulated transcript (CART; n = 24), neurotensin S (n = 2), VGF nerve growth factor-inducible protein (n = 21), calcitonin gene-related peptide (n = 4), neuromedin B (n = 4), neuromedin S (n = 2), natriuretic peptide C (n = 2) and adenylate cyclase

activating polypeptide 1 (Adcyap1; n = 2). Of these, somatostatin, galanin, cholecystokinin, neurotensin S and CART were expressed at mRNA copy numbers exceeding 100 per cell, while other peptides were found expressed at low or moderate copy numbers. mRNA transcripts for neuropeptide Y, neuromedin U, neuropeptide B and pro-opiomelanocortin were infrequently present. The co-existence of fast neurotransmitters (GABA, dopamine, glutamate) with hormones and neuropeptides allowed for a refined molecular classification of the PVN and associated hypothalamic areas (Fig. 4A,A_1).

Lastly, we focused on secretagogin mRNA expression (Fig. 4A,A_1; Table S3). From a total of 151 cells, we identified 9 cells with secretagogin mRNA transcripts. Secretagogin$^+$ cells in the sampling cohort lacked AVP, oxytocin, TRH, galanin, cholecystokinin, neurotensin S, calcitonin, neuromedin S, natriuretic peptide C and Adcyap1 mRNAs. In contrast, some secretagogin$^+$ cells contained somatostatin, Tac1, CART, neuromedin B, neuromedin U, neuropeptide Y and/or neuropeptide B mRNA transcripts (Fig. 4A,B). Secretagogin$^+$ cells abundantly carried CRH mRNA transcripts and those of the promiscuous glucocorticoid receptor NR3C1 (Fuxe et al, 1985) (Pearson correlation coefficient = 0.399, $p < 0.001$), the latter being involved in the stress-induced feedback regulation of CRH synthesis (Aguilera et al, 2007).

mRNA may not be translated into appreciable amounts of protein. Therefore, it was imperative to histochemically verify the neurochemical identity of secretagogin$^+$ neurons. First, we used a reporter mouse line expressing GFP under the control of the CRH promoter (Alon et al, 2009) to reveal the abundant presence of CRH$^+$/secretagogin$^+$ neurons in the PVN (Fig. 4C,C_1). We then applied colchicine *in vivo* to provoke neuropeptide accumulation in somatic domains in parvocellular neurons (Fig. 4D-I_2) (Cortes et al, 1990). Indeed, secretagogin was found chiefly co-expressed with CRH in PVN in both neuronal somata and local axon collaterals (Fig. 4D-E_3) and, less frequently, with tyrosine hydroxylase (ventrolateral arcuate nucleus; Fig. 4F-F_3), GABA (dorso-medial arcuate nucleus; Fig. 4G-G_2), somatostatin (Fig. 4H-H_3) and galanin (Fig. 4I-I_2) with dual-labeled secretory terminals accumulating in the median eminence (Figs. 4H and 5A-A_2). These data define secretagogin$^+$ neurons as a CRH-containing cell cohort.

Secretagogin$^+$ neurons are tightly packed in the dorsolateral PVN. Dendritic reconstructions clearly distinguish these cells from magnocellular neurons (Fig. 3C,C_1). Nevertheless, we controlled our *in vitro* transcriptome profiling by plating dissociated PVN neurons from new-born mice and assessing their dendritic morphology. Secretagogin$^+$ neurons had significantly smaller ($p < 0.05$; Fig. S2B-C) somatic diameter, more emanating ($p < 0.05$) and exceedingly arborizing ($p < 0.05$) processes than AVP$^+$ neurons. In addition, the majority were secretagogin$^+$/AVP$^-$ neurons. Yet a small secretagogin$^+$ subpopulation co-expressed AVP, with their somatic diameters and dendrite complexities reminiscent of AVP$^+$/secretagogin$^-$ neurons (Fig. S2B-C), lending further support to our *in vivo* findings (Fig. 1). Ca^{2+}-imaging experiments after KCl stimulation showed that parvocellular-like secretagogin$^+$ neurons clearly segregated from their AVP$^+$ or AVP$^+$/secretagogin$^+$ counterparts (Fig. S2D). Moreover, secretagogin$^+$ neurons

responded differentially to excitatory stimuli, including NMDA combined with glycine ($p < 0.01$), kainate ($p < 0.001$) and GABA (Haam et al, 2012) ($p < 0.001$; Fig. S3A-D_1). These data not only demonstrate that secratagogin$^+$ parvocellular neurons represent a molecularly and functionally distinct class of PVN neurons but also imply that secretagogin, a Ca^{2+}-binding protein presumed associated with the SNARE machinery *in vitro* (Rogstam et al, 2007; Bauer et al, 2011), might sculpt their responsiveness and/or affect CRH release. However, direct *in vivo* evidence discerning Ca^{2+} "buffer" *vs*. "sensor" roles for this protein remained elusive.

Secretagogin is a Ca^{2+}sensor expressed in the median eminence

Secretagogin$^+$ neurons exhibited low amplitude Ca^{2+} responses to depolarizing stimuli (Fig. S2D), as compared to AVP$^+$/secretagogin$^-$ neurons *in vitro*. Therefore, we first tested whether secretagogin acts as a Ca^{2+} buffer. Upon transfecting human SH-SY5Y neuroblastoma cells with a plasmid encoding human secretagogin we estimated their Ca^{2+} buffer capacity by population-wide (>100 cells/experiment) Ca^{2+} imaging experiments in combination with *post-hoc* assessment of neurochemical properties (Fig. S4A). The amplitude of Ca^{2+} responses in secretagogin$^+$ neurons was not statistically different from control cells (Fig. 4SB). Next, the relative level of secretagogin, scaled as immunofluorescence intensity (Fig. S4C), did not correlate with either the basal intracellular Ca^{2+} level or peak amplitudes evoked by carbachol or KCl treatments. Similarly, Ca^{2+} response kinetics failed to significantly correlate with secretagogin immunoreactivity at the level of individual cells (*data not shown*). Cumulatively, these results support that secretagogin is unlikely to function either as slow or fast Ca^{2+} buffer, at least *in vitro*.

In view of the negative data on Ca^{2+} buffering, we hypothesized that secretagogin is a Ca^{2+} sensor *in vivo*. This notion is supported by secretagogin's concentration and co-localization with CRH in the median eminence (Fig. 5A-A_2), the locus of the first capillary network of the hypothalamic artery that collects releasing hormones produced by neurosecretory cells, including CRH (Harris, 1972; Swanson et al, 1983). In particular, we employed pre-embedding silver-intensified immunogold labeling to show, at the ultrastructural level, that secretagogin is present in axon terminals with frequent association to the plasmalemma, and possibly also to the outer membrane of dense-core vesicles (Fig. 5B,B_1; for quantitative data in axons see Fig. 2D). The presence of silver precipitates along the inner membrane of the nerve terminal reinforces a potential role for secretagogin as a Ca^{2+} sensor.

Next, we addressed if secretagogin is a Ca^{2+} sensor to influence neurotransmitter transport and vesicular release by defining its Ca^{2+}-dependent interactome using unbiased matrix assisted laser desorption ionization-time of flight (MALDI-TOF) proteomics (Fig. 5C). We deployed a subtractive approach, whereby positive hits were defined as only recruited in the presence of 10 μM Ca^{2+} in the isolation buffers but not recovered under Ca^{2+}-free conditions or by non-specific rabbit IgGs. Our hits (97 proteins in Ca^{2+}-dependent interactions and 15 proteins without Ca^{2+} dependence (Table S4); minimum number of peptide fragments ≥2, protein threshold: 99%,

peptide threshold: 99%) therefore were interpreted as recruited upon Ca^{2+} influx (Fig. $5C_1$, Table S4), and chiefly included proteins implicated in *i*) vesicle formation, fusion and traffic, *ii*) enzymatic reactions, *iii*) signaling, and *iv*) cytoskeletal dynamics and axonal transport (Fig. $5C_1$) (Sudhof, 2004; Schluter et al, 2006; Wickner et al, 2008). We also uncovered interactions with other Ca^{2+}-binding proteins, glutamate decarboxylase and vesicular GABA transporter (Fig. $5C_1$), reinforcing our transcriptome analysis. We validated the expression of mRNAs for many of these proteins in secretagogin$^+$ neurons by targeted analysis of our single-cell transcriptome data (Fig. 5D). This approach revealed the expression of multiple genes of interest involved in vesicular traffic and fusion in secretagogin$^+$ parvocellular neurons (Fig. 5D). Lastly, we performed immunohistochemistry in rat paraventricular neurons and median eminence with antibodies raised against Rab3 (all isoforms) to visualize secretagogin's frequent co-existence with this family of proteins at the median eminence (Fig. $5E\text{-}E_3$). In sum, these findings suggest that secretagogin is a Ca^{2+} sensor, which can affect CRH release from parvocellular neurons.

Secretagogin controls CRH release *in vitro* and *in vivo*

We first determined whether secretagogin can affect CRH release by its RNAi-mediated knock-down in native PVN neurons (Fig. 6A), followed by secretagogin histochemistry and the recovery of CRH in culture supernatants (Fig. $6A_1$). We found significantly decreased CRH content in the culture media of hypothalamic neurons exposed to secretagogin-directed RNAi (Fig. $6A_1$). Subsequently, we took the opposite approach and transiently overexpressed secretagogin in an immortalized CRH-containing embryonic mouse hypothalamic cell line (mHypoE-N44). Three days after transfection, mHypoE-N44 cells were stimulated with 15 µM ATP for 20 min, fixed, and immunostained for secretagogin (Fig. $6B,B_1$) with simultaneous intracellular CRH detection (Fig. $6B_2$). CRH levels negatively correlated with that of secretagogin (Pearson's correlation coefficient = -0.189, p = 0.016) upon secretagogin overexpression. In contrast, no significant correlation between cytosolic secretagogin and extracellular CRH content was determined in non-stimulated samples (Pearson's correlation coefficient = 0.0379, p = 0.56). We concluded that in mHypoE-N44 cells secretagogin can facilitate ATP-dependent CRH release without an effect on CRH synthesis *per se*.

Next, we sought evidence that secretagogin knock-down affects CRH release *in vivo* by injecting siRNA ("Accell") against secretagogin into the lateral ventricle and by performing quantitative double-label histochemistry in serial sections 3 days later. In the anterior PVN, which comprises CRH$^+$ parvocellular neurons (Keegan et al, 1994), secretagogin knock-down occurred in 20-30% of CRH neurons (Fig. $6C,C_1$). Since CRH, like other neuropeptides, undergoes axonal transport and Ca^{2+}-dependent release after synthesis (Alonso et al, 1986), we observed CRH retention in parvocellular neuronal somata in PVN in RNAi-exposed hypothalami (p < 0.05; Fig. $6C_2,D,D_1$). We attributed the lack of change in secretagogin immunoreactivity, when measuring immunofluorescence intensity in individual cells, to the fact that our knock-down approach effectively arrested secretagogin expression in high CRH-expressing neurons, as supported by the relative scarcity of dual-labeled neurons. We

considered our RNAi approach aimed to silencing secretagogin expression specific because neither magnocellular neurosecretory cells nor some neuropeptide systems localized to the PVN were affected upon experimental manipulations (Fig. S5A-D). Overall, our data suggest that secretagogin might modulate CRH release in the hypothalamus.

Secretagogin gates the CRH-ACTH axis in response to acute stress

Secretagogin's involvement in modulating CRH release *in vitro* and *in vivo* suggests that this Ca^{2+}-binding protein can be instrumental to modulate the stress-induced mobilization of the hypothalamo-pituitary-adrenal axis by priming the hierarchical CRH-ACTH cascade that underpins a peripheral corticosterone surge from the adrenal cortex (Swanson et al, 1980; Makara et al, 1981; Swanson et al, 1989). If so, secretagogin$^+$ neurons are assumed to rapidly up-regulate their CRH content and function as "on-neurons" to activate hormonal responses to stress. We addressed this hypothesis by injecting formalin (4%) into one paw (Pacak et al, 1995; Naveilhan et al, 2001) and detecting activation of the immediate early gene c-fos (Ohtori et al, 2000) in the PVN 6h later (Fig. 7A,B). Quantitative immunohistochemistry revealed that 62 ± 8% of c-fos$^+$ neurons co-expressed secretagogin and CRH (Fig. 7B$_1$).

Since secretagogin is a Ca^{2+} sensor protein expressed in CRH$^+$ cells recruited by acute stress, it is plausible to assume that its physiological role is the control of CRH release. To test this hypothesis, we performed secretagogin siRNA knock-down *in vivo* followed by determination of circulating ACTH and corticosterone levels 12 minutes after evoking formalin stress, coinciding with peak ACTH responses in blood (Cam et al, 1983). Formalin injection in control animals (that is, injected with non-target siRNA 4 days prior) produced significant increase in ACTH content in plasma (Fig. 7C). In contrast, infusion of secretagogin-specific siRNA into the lateral ventricle 4-days prior to formalin challenge blunted this ACTH response ($p < 0.05$; Fig. 7C). Likewise, the ensuing corticosterone response was significantly reduced (Fig. 7D) in mice treated with secretagogin siRNA. In sum, our data suggest that secretagogin is instrumental for CRH release and stress responsiveness.

Discussion

This study provides novel insights in the neurochemical organization of the mammalian hypothalamus. We report that secretagogin in many parvocellular neurons modulates CRH release. Unlike for small neurotransmitters, CRH, as many other hormones, is not reused or recycled at the locus of its release. Moreover, CRH is transported over considerable distances from its somatic site of synthesis in the PVN to the median eminence (Fig. S6). Thus, hormonal secretion into the bloodstream is reliant on the coordination of regulated checkpoints, which might either be indirectly (vesicle formation and axonal transport; Fig. S6A) or directly (vesicular exocytosis) affected by secretagogin. From a technical stand-point, our study uses an interactive design of single-cell transcriptome and proteome discovery, verified at the level of systems neurobiology. Yet we did not apply real-time imaging of CRH release upon genetic

manipulation of secretagogin expression. Therefore, we cannot entirely exclude that secretagogin, at least in part, primes the release machinery indirectly by recruitment of a multicomponent apparatus rather than directly interacting with its key components (Fig. S6B). Nevertheless, secretagogin was identified as a Ca^{2+} sensor protein whose proteome-wide interactions include α-SNAP, Rab family members, syntaxins, synaptophysin, TMED10 and CAPS1, many of which were implicated in vesicle formation, trafficking, exo- and endocytosis, and are integral components of synaptic vesicle membranes (Takamori et al, 2006; Tobin et al, 2012a; Tobin et al, 2012b). These interactions are compatible with the predominant association of secretagogin with the plasmalemma and endomembranes in hypothalamic neurons and nerve endings in the median eminence. We hypothesize that differential distribution of secretagogin in axons is due to the fusion of somatic endomembranes into the axonal plasma membrane, thus providing a structural conduit for secretagogin trafficking towards exocytosis release sites. Besides, secretagogin's Ca^{2+}-dependent interactions include molecular motors (kinesin-1, myosin-10), with kinesin-1 known to affect axonal transport (Hirokawa et al, 2005), suggesting that secretagogin can intracelluarly modulate the timing and velocity of cargoes moved along the axon and readied for subsequent exocytosis.

Although detailed neuroanatomy studies define at least 7 neurochemically-distinct sub-regions of the mammalian PVN (Simmons et al, 2009), the classical cytoarchitectonic concept is that dorso-laterally located magnocellular neurons are spatially segregated from the parvocellular cell groups. While parvocellular neurons concentrate between the 3rd ventricle and magnocellular neuron clusters, CRF neurons neighbor magnocellular neurosecretory cells along the ventro-lateral extremity of this hypothalamic area (Swanson et al, 1980; Swanson et al, 1983; Pelletier, 1991). This cytoarchitectonic organization is derived from a string of exquisite neuroanatomical studies spanning the past ~40 years (Kiss et al, 1983; Palkovits, 1984; Swanson et al, 1986; Kita et al, 1986; Swanson et al, 1989; Swanson, 1991; Horvath et al, 2005; Simmons et al, 2009; Maejima et al, 2009; Vogt et al, 2014) and utilizing hormones/neuropeptides to mark neurosecretory cell identity, as well as somatic size measurements as classification criteria (Kiss et al, 1991). These classical methods often relied on colchicine-treated or stressed rodents to provide unequivocal phenotypic information on, e.g., CRH neurons. Under these conditions, CRH cells co-express additional hormones and peptides, including vasopressin, neurotensin, angiotensin II and encephalin (Swanson et al, 1986; Ceccatelli et al, 1989). With regard to fast neurotransmitters, CRH neurons in rat are mainly glutamatergic (Hrabovszky et al, 2005) even though a subgroup was shown to be GABAergic (Meister et al, 1988). Functionally, the action of amino acid neurotransmitters to modulate pituitary hormone-producing endocrine cells may occur *via* local axon collaterals within the PVN. Local amino acid transmitter synthesis in, and release from, nerve endings in the external layer of the median eminence may yet modulate the release of CRH (and other releasing/inhibitory factors) into portal vessels by engaging presynaptic auto- and/or heteroreceptors.

The advent of single-cell transcriptome analysis by RNA-sequencing (Shapiro et al, 2013) revolutionized insights in cell diversity in many developing (Tang et al, 2009) and adult tissues (Islam et al, 2011; Kodama et al, 2012; Lovatt et al, 2014). In the nervous system, transcriptome analysis is predicted to reveal that neuronal diversity is far more complex than initially thought, with many non-classical neuronal sub-types emerging (that is, modalities or combinations of the mRNA landscape overarching several known cell subsets). These might be of particular relevance to specific behavioral contexts, environmental challenges or disease phenotypes. More specifically, in the mammalian hypothalamus, a significant expansion of the phenotypic divergence of functionally distinct neuroendocrine subtypes, carrying mixed phenotypic codes including sub-threshold levels of hormones or neuropeptides, is expected upon unbiased clustering of cellular transcriptomes. This will identify neuroendocrine cell cohorts differentially responding to not one but multiple stimuli. As such, secretagogin^{+} neurons in mouse were found to express mRNA transcripts for Crh, Gad1, Gad2, Slc32a1, Tac1 and somatostatin. This mRNA transcript repertoire confers, as said, a parvocellular origin (Dierickx et al, 1979; Alonso et al, 1986; Ceccatelli et al, 1989); yet with a broader mRNA spectrum than for a single classical subtype of parvocellular neuroendocrine cells. These considerations cumulatively have the following inferences: parvocellular neurons express a chief hormone, a neuropeptide. Nevertheless, they maintain the ability to co-express other (secondary) releasable products, including small molecule transmitters such as GABA and glutamate playing auxiliary roles. This allows dynamically switching mode of action upon a range of metabolic stimuli, underpinning fast “on/off” responses. Here, this hypothesis is reflected by the moderate presence of secretagogin in magnocellular neurons and their axon terminals in the posterior pituitary. Moreover, our single-cell transcriptome analysis revealed the coincidence of Scgn, Crh and Nr3c1 mRNA expression. *Nr3c1* encodes a glucocorticoid receptor (nuclear receptor subfamily 3, group C member 1) (van Rossum et al, 2004). NR3C1 can both function as a transcription factor that binds to glucocorticoid response elements in the promoters of glucocorticoid responsive genes to activate their transcription or act as a regulator of other transcription factors. *Nr3c1* mutations manifest as generalized glucocorticoid resistance (Donner et al, 2013), characterized by the insensitivity of target tissues to glucocorticoids, resulting in the compensatory activation of the HPA axis and CRH hypersecretion into the systemic circulation. Thus, secretagogin may be the first molecular hinge linking NRC31-mediated feedback to CRH release from parvocellular neurons.

Since parvocellular neurons receive local-circuit, as well as long-range afferents (Kiss et al, 1984; Palkovits, 1987; Kiss et al, 1996), the predominance of single gene products coincides with, and is driven by the type of excitatory or inhibitory inputs they receive. Considering that hypothalamic neuronal circuitries are prone to synaptic reorganization upon metabolic challenges (Pinto et al, 2004; Horvath et al, 2005), parvocellular neurons might function as “fast integrators” in hypothalamic neuronal circuitries, and can translate synaptic information into hormonal output with high fidelity. This arrangement is compatible with our electrophysiology classification showing that secretagogin^{+} neurons, although clearly parvocellular, belong to both

Ia and *IIa* PVN subclasses. In addition, an evolutionary advantage of the broad functional diversity of neuronal contingents in the hypothalamus may be the ability of sustained neural control of secondary metabolism at the periphery, essential for the survival of the organism, even under pathological conditions associated with neuronal loss.

Action potentials represent the temporal code of electrical activity in neurons. Upon the arrival of a depolarization wave, a kaleidoscope of voltage-dependent ion channels regulates ion exchange along the plasma membrane. On the one hand, this influx of Ca^{2+} is to induce signaling events shaping the neurons' transcriptional program to adapt to circuit requirements (Clapham, 2007). On the other hand, Ca^{2+} is the ubiquitous trigger for the quantal release of neurotransmitters and neuromodulators at axon terminals (Sudhof, 2004). In the hypothalamus, intracellular Ca^{2+} signaling regulates AVP and oxytocin release in magnocellular neurons (Dayanithi et al, 2012). Parvocellular neurons are equally dependent on Ca^{2+}-dependent mechanisms (Hallbeck et al, 1996). In particular, a Ca^{2+}/calmodulin-dependent signaling pathway was reported to modulate the transcription of CRH in neurons (Yamamori et al, 2004). Ca^{2+} waves are transduced into intelligible second messenger codes by Ca^{2+} sensor proteins with low affinity (> 1 μM) in protein-protein interactions. Alternatively, cytosolic Ca^{2+} buffers (Ca^{2+} affinity; < 1 μM) dissipate Ca^{2+} transients by reversibly binding 2-6 Ca^{2+} ions (Andressen et al, 1993). Although a clear separation of these two protein subfamilies is increasingly debated (Schwaller, 2009), a clear evidence for Ca^{2+} sensor function is the Ca^{2+}-dependent recruitment of signaling proteins. Here, we used subtractive proteomics to define the Ca^{2+}-dependent interactome of secretagogin in native hypothalamic preparations. Our data revealed that secretagogin interacts with protein subfamilies implicated in the formation, intracellular traffic, priming and docking of release vesicles. These findings are not entirely unexpected, since a pull-down analysis using purified secretagogin as bait reported similar results (Bauer et al, 2011). However, this is the first confirmed report of secretagogin's interactome *in situ* in an identified neuronal cohort, which defines cell type-specific protein interactions for this Ca^{2+} sensor. Critically, our single-cell transcriptome data confirmed the presence of mRNAs for the proteins identified by mass spectrometry, providing unbiased support for our functional assays. The above data together with secretagogin's localization in giant axon terminals at the median eminence, and its association to the readily-releasable pool of vesicles, as well as plasmalemmal compartments in the vicinity of release sites, show that secretagogin is ideally poised to gate neuropeptide secretion. Considering that secretagogin$^-$ nerve endings also exist in the median eminence, our results also suggest that as yet unknown and additional Ca^{2+}-dependent or independent sensor proteins might exist to control the release of hormones distinct from CRH, galanin or somatostatin (Fig. 5).

A primary drive of molecular neuroscience is the discovery of signaling events rate-limiting neural processes indispensable for the formation, maintenance and responsiveness of key neural axes. We demonstrated that acute noxious stress increases CRH expression in the PVN, particularly in secretagogin$^+$ neurons. A causal relationship between secretagogin expression

and CRH release is cumulatively highlighted by gain-of-function and loss-of-function analysis employing the coincident detection of the intracellular candidate (secretagogin) and the physiological output (CRH in media). Based on our protein interactome profiling, cell biology and neuroanatomy analyses, we propose that genetic impairment of secretagogin expression disrupts the traffic of CRH-laden neurosecretory vesicles towards release sites, as shown by the somatic accumulation of CRH immunoreactivity upon siRNA-mediated secretagogin silencing *in vivo*. Most notably, genetic manipulation of secretagogin availability led to the fall-out of stress-induced ACTH elevation in peripheral blood, which is normally driven by the activation of CRH receptors on secretory cells of the anterior pituitary (Wynn et al, 1983). Whilst ACTH expression is a multifactorial mechanism (Armario, 2006), we argue that the blunted ACTH response was due to the experimentally evoked attenuation of CRH release at the median eminence. Nevertheless, corticosterone release in stressed animals was only partially suppressed. This may be due to our coincident ACTH and corticosterone sampling protocol focused on the primary ACTH response, and only capturing a relatively early up-shoot in the plasma corticosterone concentration.

Overall, we show that a spatially-segregated parvocellular neuron population produces CRH, and regulates its release *via* a novel Ca^{2+} sensor. Therapeutic implications of these findings are vast, since they offer novel biomarkers for some of the most common metabolic disorders, and druggable targets for ceasing CRH release particularly in chronic stress, depression and genetic or sporadic forms of generalized glucocorticoid resistance.

Experimental Procedures

Animals for histo- and biochemistry

Histochemical, biochemical and *in vivo* RNAi experiments were conducted in male C57BL/6N mice (*n* = 57, 12 weeks of age) and Sprague Dawley rats (*n* = 7; both from Scanbur). CRH-EGFP reporter mice (all females, *n* = 3, 19 weeks of age) were generated using bacterial artificial chromosome technology (Alon et al, 2009). Hypothalamic cultures were prepared from mouse pups on postnatal day (P)2. Animals were housed conventionally (12/12h light cycle, 25% humidity). Adult mice (*n* = 4) received stereotaxic injections of colchicine (5 µl; Sigma) into the left lateral ventricle under deep anaesthesia (5% isoflurane) and survived for an additional 24h to facilitate somatic neuropeptide accumulation (Cortes et al, 1990). Experimental protocols were in accordance with the European Communities Council Directive (86/609/EEC) and approved by the regional ethical committee (Stockholms Norra Djurförsöksetiska Nämnd; N512/12). Particular effort was directed to minimize the number of animals and their suffering during the experiments.

Tissue preparation, immunohistochemistry and imaging

Wild-type animals were transcardially perfused with a fixative composed of 4% paraformaldehyde (PFA) in 0.1M phosphate buffer (PB, pH7.4) that was preceded by a short prerinse with physiological saline (anesthesia: 5% isoflurane). CRH-EGFP mice were perfused with 0.1M phosphate-buffered saline (PBS; 37 ^{o}C, pH7.4) followed by 4% PFA in 0.1M PBS (37 ^{o}C [20 ml] switched to ice-cold [50 ml]). After post-fixation in the same fixative overnight and cryoprotection in 30% sucrose for at least 48h, 30 or 50 µm-thick serial sections were cut on a cryostat microtome and processed for multiple immunofluorescence histochemistry according to published protocols (Mulder et al, 2009). Alternatively, perfused brains were cryoprotected in 10% sucrose and sectioned onto SuperFrost^{+} glass slides at 20 µm thickness.

Free-floating sections were rinsed in PB (pH 7.4) and pre-treated with 0.3% Triton X-100 (in PB) for 1h at 22-24 °C to enhance the penetration of antibodies. Non-specific immunoreactivity was suppressed by incubating our specimens in a cocktail of 5% normal donkey serum (NDS; Jackson), 1% bovine serum albumin (BSA; Sigma) and 0.3% Triton X-100 (Sigma) in PB for 1h at 22 - 24 °C. Sections were then exposed to select combinations of primary antibodies diluted in PB to which 0.1% NDS and 0.3% Triton X-100 had been added for 16 - 72h at 4 °C (Table S2). After extensive rinsing in PB, immunoreactivities were revealed by carbocyanine (Cy)2, 3 or 5-tagged secondary antibodies raised in donkey (1:200; Jackson; 2h at 22 - 24 ^{o}C). Sections were mounted onto fluorescence-free glass slides and coverslipped with Entellan (in toluene; Merck).

Double labelling of glass-mounted sections with the tyramide signal amplification Plus method (Shi et al, 2012) (TSA; Perkin-Elmer) combined with the use of Cy2-conjugated secondary antibodies was performed as described. Glass-mounted sections were coverslipped with Aquamount (Dako). Images were acquired on Zeiss 700LSM, 710LSM or 780LSM confocal

laser-scanning microscopes with maximal signal separation or spectral scanning. Composite figures were assembled in CorelDraw X5.

Electron microscopy

Male C57Bl6/J mice (*n* = 8) were anesthetized with pentobarbital (50 mg/kg) and transcardially perfused with physiological saline followed by 4% PFA and 0.25% glutaraldehyde in PB for 15 min. After removal of the brain, a diencephalic block was trimmed and cut in 100-µm frontal sections on a VT1200S vibratome (Leica). Sections containing the anterior hypothalamus were collected and immersed in 4% PFA in PB for an additional 2h. Specimens were optionally stored in a mixture of 10% glycerol and 25% sucrose at -80 °C. For ultrastructural analysis, sections were thawed, rinsed in PB (3x) and then incubated in 0.1M Tris-NaCl buffer supplemented with 0.1% Tween-20 (TNT), 1% BSA and 1% glycine for 30 min. This was followed by exposure to anti-secretagogin antibodies (1:2,000 (L.W.), 1:800 (Sigma) in PB-TNT-BSA; Table S2) at 4°C overnight. Sections were then rinsed in the above buffer and incubated with goat anti-rabbit F(ab')$_2$-coupled to 0.8 nm gold particles (1:100; Aurion) in PB-TNT-BSA for 2 h at 22-24 °C. After fixation with 1% glutaraldehyde (10 min) and rinsing in water, gold particles were Ag-enhanced using the HQ Silver Enhancement Kit (Nanoprobes; 5 min at 22-24 °C) prior to post-fixation in 1% OsO_4 for 1h. Next, sections were flat-embedded (Epoxy resin) between two plastic coverslips. After polymerization, regions of interest were identified under a stereomicroscope, isolated with a razor blade and re-embedded in Epon. Ultra-thin sections (60 nm) perpendicular to the thickness of the vibratome section were obtained and optionally contrasted by uranyl-acetate and lead citrate. Specimens were finally observed by using an H7650 Hitachi electron microscope.

The number of silver-enhanced gold particles in neuronal profiles of three compartments (that is, soma, dendrites and axonal nerve endings) in the PVN and external median eminence were quantified. In every compartment, we determined the distribution of these particles in a membrane-related domain (either the plasma- or an endomembrane) and in a cytosolic domain where no obvious organelle could be detected underneath. For this purpose, we measured the distance between particles and membranes on photomicrographs from *n* = 5 mice, and considered a particle membrane bound if its distance was <50 nm from the closest membrane profile. The number of counted profiles was as follows: soma: plasma membrane = 25; endomembrane = 29; cytosol = 27; dendrite: plasma membrane = 24; endomembrane = 21; cytosol = 15; axon: plasma membrane = 28; endomembrane = 25; cytosol = 25. Data were expressed as the number of particles per neuronal profile ± s.e.m.

Patch-clamp electrophysiology

Male C57Bl6/N mice (*n* = 22; 21-28 days) were deeply anesthetized (5% isoflurane) and decapitated. Brain were rapidly removed and immersed in ice-cold pre-oxygenated (95% O_2/5% CO_2) cutting solution containing (in mM): 90 NaCl, 26 $NaHCO_3$, 2.5 KCl, 1.2 NaH_2PO_4, 10 Hepes-NaOH, 5 Na-ascorbate, 5 Na-pyruvate, 0.5 $CaCl_2$, 8 $MgSO_4$ and 20 glucose.

Subsequently, 300 µm-thick coronal slices were cut on a vibratome (VT1200S, Leica). Slices encompassing the PVN region were selected and equilibrated in artificial cerebrospinal fluid (ACSF) containing (in mM): 124 NaCl, 26 $NaHCO_3$, 2.5 KCl, 1.2 NaH_2PO_4, 2 $CaCl_2$ and 2 $MgSO_4$ at 22-24 ^oC for 1 - 5 h before recording. Whole-cell recordings in current-clamp or voltage-clamp mode were made by using a HEKA ECP-10USB amplifier and PatchMaster Software (HEKA, Germany). During measurements, slices were continuously perfused with ASCF. The internal pipette solution contained (in mM): 114 K-gluconate, 6 KCl, 10 HEPES, 5 EGTA, 4 ATP-Mg, 0.3 GTP (pH was adjusted to 7.3 with KOH) and 0.5% biocytin (Sigma) for *post-hoc* cell identification. After recordings, brain slices were immersion fixed with 4% PFA at 4°C overnight. Electrophysiological data were analyzed using Clampfit 10.0 (Molecular Devices) and SigmaPlot (Systat Software Inc.) for the parameters listed in Table S1.

Single cell transcriptome analysis

The PVN region of juvenile mice was isolated from 300 µm-thick coronal slices under microscopy guidance and dissociated using the Papain Dissociation System (Worthington). Isolated single cells were concentrated by centrifugation to a density of 300 - 500 cells/µl, and load into a C1-AutoPrep system (Fluidigm) for single cell capture, lysis, cDNA synthesis and amplification (Islam et al, 2014). Each capture site was imaged with 192 cells selected for RNA-sequencing on an Illumina HiSeq2000 sequencer. Sequencing data at a depth of 500,000-2,000,000 reads/cell were analyzed (Islam et al, 2014). Out of 151 confirmed single cells, 130 cells provided data above a threshold of 10,000 transcript molecules/cell (excluding repeats and mitochondrial transcripts). Data on molecule counts were next subjected to clustering. In brief, ~2,700 genes were selected based on their expression (average more than one molecule/cell and correlation > 0.5 with other 10 genes). Based on these criteria, the 1D order of cells and genes was performed using the SPIN Neighborhood algorithm (Tsafrir et al, 2005).

Immunoprecipitation & unbiased proteomics

Hypothalamic regions containing the PVN were isolated from P7 rats (3 animals), divided into left and right parts with one heimsphere incubated in ACSF ("control stimulation"), while another placed in ACSF in which 52.5 mM NaCl was replaced by KCl to depolarize neurons by inducing Ca^{2+} influx ("treatment condition"). After 10 minutes of incubation, samples were collected in lysis buffer containing 50 mM NaCl, 20 mM HEPES, 10 µM $CaCl_2$, 1 mM EDTA, 0.2% Triton X-100 and a cocktail of protease inhibitors (Roche; pH was adjusted to 7.4). Meanwhile, samples treated by depolarizing solution were transferred into the above lysis buffer supplemented with 10 µM $CaCl_2$ without EDTA. Tissues were homogenized, centrifuged at 14,000 *rpm* for 30 min and supernatants used in subsequent experiments. After pre-clearance, samples were incubated with rabbit anti-secretagogin primary antibody (1:2,000; provided by L.W.) overnight at 4 °C. An aliquot of each sample was exposed to rabbit IgG (Santa Cruz Biotechnology) to control non-specific binding. Subsequently, samples were incubated with GammaBind Plus Sepharose beads (GE Healthcare) for 90 min. After repeated rinses, proteins were eluted with

Laemmli buffer and separated on 10% SDS-PAGE under denaturing conditions. After silver in-gel staining, proteins in each lane were identified by matrix-associated laser desorption ionization time of flight mass spectrometry (Proteomics Science Facility at Karolinska Institutet) (Linden et al, 2012). The MS/MS data file generated was analysed using the Mascot algorithm (Version 2.5, Matrix Science) against the NCBInr database selected for rat (*Rattus norvegicus*) taxonomy, trypsin as the cleavage enzyme, carbamidomethyl as a fixed modification of cysteines and methionine oxidation and then deamidation of glutamines and asparagines as variable modifications (Tortoriello et al, 2014). All of the three 'pool' mgf files within each treatment were merged before searching. Peptides were selected with a fragment tolerance of 0.1 Da and parent tolerance of 0.05 Da, and with a confidence threshold of >99%. Proteins were unambiguously identified with 2 or more peptides and a protein threshold of >99%. Additional data analysis was performed using Scaffold (Version 4.3.4).

Cell culture and secretagogin manipulation

Human SH-SY5Y neuroblastoma cells and embryonic mouse hypothalamic cell line N44 (mHypoE-N44; Cedarline®) were seeded at a density of 50,000 cells/well on poly-D-lysine (PDL)-coated 24-well plates and cultured in DMEM:Glutamax (Invitrogen) containing 10% fetal bovine serum overnight (without antibiotics). Lipofectamine 2000 (2 µl/well; Invitrogen) was used to transfect both cell lines with a pcDNA3.1 plasmid containing the human *scgn* gene (0.5 µg/well). Forty eight h after transfection, the cells were used for Ca^{2+} imaging and *post-hoc* immunocytochemistry. mHypoE-N44 cells were routinely serum-starved for 1 day in DMEM:Glutamax also containing 25 µM forskolin. Subsequently, cells were stimulated by ATP (15 µM) for 20 min before immersion fixation in 4% PFA in PB.

Hypothalami of mice were isolated on ice after decapitation on P2. After enzymatic dissociation, cells were plated at a density of 300,000 cells/well in PDL-coated 24-well plates, and grown for 7-8 days *in vitro* (DIV). For Ca^{2+} imaging, 50,000 cells were plated in each well. Cultures were maintained in DMEM/F12 containing B27 supplement (2%), L-glutamine (2 mM), penicillin (100 U/ml) and streptomycin (100 mg/ml; all from Invitrogen). For *post-hoc* immunocytochemistry, cells on coverslips were fixed in 4% PFA for 30 min on ice, and subsequently immunostained using select combinations of primary antibodies (Table S2). Parameters processed for quantitative morphometry of single and dual-labelled cells included: *i*) the somatic diameter, *ii*) number of neurites, *ii*) the maximum length of processes and *iv*) the number of neurite branching ("bifurcations"; Fig. S2C; for analysis procedures see: (Keimpema et al, 2010)). For secretagogin knock-down, primary hypothalamic neurons were grown for 4 days *in vitro* followed by exposure to 1 µM Accell secretagogin-specific siRNA (Thermo Fisher) for an additional 3 days. CRH release was determined after adding fresh medium containing 25 µM forskolin (Sigma) and incubation for 18h by ELISA detection (CusaBio).

Ca^{2+} imaging and quantitative immunocytochemistry

Ca^{2+} responses were measured using Fura-2AM (Invitrogen) as intracellular Ca^{2+} indicator. Ratiometric imaging was performed on a CoolSnap HQ^2 camera (Photometrics) and analyzed by MetaFluor software (Mollecular Devices). After recording, the cells on coverslips were immersed in ice-cold 4% PFA in PB, and processed for immunocytochemistry as above. For quantitative immunocytochemistry (fluorescence densitometry), orthogonal z-stacks were captured on an LSM700 laser-scanning microscopy (Zeiss). Fluorescent intensity of single cells was determined by using the ImarisPro software (Bitplane), and correlated with corresponding Ca^{2+} responses (Figs. S3 & S4).

***In vivo* stress and siRNA-mediated secretagogin knock-down**

First, we tested whether formalin-stress induces c-fos accumulation in secretagogin $^+$ PVN neurons by subcutaneous injection of 4% PFA (50 µl). After 6h, mice (*n* = 2/time point) were transcardially perfused as above, and their PVN processed for multiple immunofluorescence detection of c-fos, secretagogin and CRH (Table S2). The number of c-fos^+, $secretagogin^+$ and c-fos^+/$secretagogin^+$ neurons were counted in 8,000-18,000 μm^2 frames superimposed over the PVN (ZEN2010 software, Zeiss). C-fos^+ nuclei were only counted if their fluorescent intensity exceeded tissue fluorescence by >4-fold.

Second, the contribution of secretagogin in stress-induced hormone release *in vivo* was assessed in male mice (*n* = 24, 12 weeks of age). Animals (*n* = 12) received stereotaxic injections of either 250 µM SMARTpool Accell Scgn siRNA (1nmol; Thermo Fisher Scientific) or Accel non-targeting siRNA (*n* = 12) in the left lateral cerebral ventricle (4 µl). A recovery period of 96h was used before stress induction. Formalin stress was induced by injection of 4% PFA into the left paw. Blood (*n* = 24) was collected with a lag-time of 12 min at the expected peak of circulating ACTH.

Third, the quantitative analysis of secretagogin knock-down efficacy was performed by analyzing the distribution and fluorescence intensity of CRH^+ neurons in the PVN after *in vivo* knock-down as above with 2 µl of either 250 µM SMARTpool Accell Scgn siRNA (0.5 nmol; *n* = 3) or Accel non-targeting siRNA (*n* = 3). After transcardial perfusion and immunohistochemistry, projection images of orthogonal *z*-stacks (interval depth: 2 µm, optical thickness: 2 µm) were analyzed using the maximal intensity projection function of the ZEN2010 software (Zeiss; Fig. 6C,C_1).

ACTH concentrations were determined in unextracted plasma samples using a radioimmunoassay (RIA). Synthetic human ACTH1-39 was used as standard and for labeling with ^{125}I (I-RB-4, Institute for Isotopes, Budapest, Hungary). An ACTH antibody (no. 8514), directed against the mid-portion of the human ACTH1-39 molecule, was raised in rabbit at the Institute of Experimental Medicine, Hungarian Academy of Sciences (Budapest, Hungary) (Barna et al, 1992). This antibody is highly specific, showing 0.2% cross-reaction with α-MSH,

and no significant cross-reaction with γ-MSH, CLIP, ACTH11-24, ACTH25-39, ACTH1-14, and ACTH1-19. The intra- and inter-assay coefficients of variation were 4.7 and 7%, respectively.

Plasma corticosterone was measured from 10 µl of unextracted plasma with an RIA by use of a specific antiserum (Institute of Experimental Medicine, Hungarian Academy of Sciences) against corticosterone-3-carboxymethyloxim-BSA. An ^{125}I-labeled carboxymethyloxim-tyrosine methyl ester derivative was used as tracer (I-RBO-36, Institute for Isotopes, Budapest, Hungary). The corticosterone antibody only cross-reacts with other naturally occurring adrenal steroids at <0.05%, except desoxycorticosterone (1.5%) and progesterone (2.3%). Final dilution of the antibody was 1:40,000. Incubation time was 24 h at 4°C, and a second antibody (anti-rabbit from goat) and 6% polyethylene glycol were used for separation. A calibration curve was prepared from corticosterone (Calbiochem), ranging from 0.27 to 40 pmol/tube. The intra- and interassay coefficients were 12.3 and 15.33%, respectively. All hormone measurements were performed in duplicate.

Statistical analysis

Data were analyzed using Statistical Package for the Social Sciences (version 21.0, SPSS Inc.) and SigmaPlot (Systat Software Inc.). Data were expressed as means ± s.e.m. A p value of < 0.05 was considered statistically significant, and calculated by Student's *t*-test (on independent samples), Mann-Whitney rank sum test or one-way analysis of variance (ANOVA with Dunn's *post-hoc* test), as appropriate.

Acknowledgments & Funding Statement

The Authors thank T.L. Horvath (Yale School of Medicine) and L. Swanson (University of Southern California) for their critical comments on this manuscript. Lisa E. Pomeranz and Kaamashri N. Latcha (The Rockefeller University) are acknowledged for providing brain tissues from CRH-EGFP mice. The expert technical assistance of Mrs. Eva Dobozi Kovacs is greatly appreciated. The Authors also thank the Bordeaux Bioimaging Center (CNRS UMS 3420) for technical support. This work was supported by the Swedish Research Council (T.Ha., T.Hö.), Hjärnfonden (T.Ha.), the Petrus and Augusta Hedlunds Foundation (T.Ha., T.Hö.), the Novo Nordisk Foundation (T.Ha., T.Hö), the Karolinska Institutet (T.Hö.), the Medical University of Vienna (T.H.), ANR (France, ANR-10-INBS-04-01, M.L.), the European Commission (PAINCAGE grant, T.H.) and the Wellcome Trust (094476/Z/10/Z, equipment grant, C.H.B. and postdoctoral research fellowship, M.F.).

Legends to Figures

Figure 1 Secretagogin locus in the paraventricular nucleus of the hypothalamus.

(**A-A$_3$**) Secretagogin$^+$ neurons populate the paraventricular, dorsolateral, ventromedial, periventricular and arcuate nuclei of the mouse hypothalamus (Paxinos et al, 2001). Red circles denote the localization of neuronal perikarya and their relative densities. *Abbreviations*: AHP, anterior hypothalamus; Arc, arcuate nucleus; DM, dorsomedial nucleus of the hypothalamus; ME, median eminence; Pe, periventricular nucleus of the hypothalamus; PVN, paraventricular nucleus, PVNm, magnocellular part; SON, supraoptic nucleus; VM, ventromedial hypothalamic nucleus.

(**B-B$_2$**) Largely non-overlapping distribution of AVP-positive($^+$). oxytocin$^+$ and secretagogin$^+$ (sgcn$^+$) neurons in the magnocellular PVN. The mouse supraoptic nucleus (SON) harbored vasopressin$^+$ and oxytocin$^+$ but not secretagogin$^+$ neurons. *Open arrowheads* pinpoint single-labeled neurons. Solid arrowhead denotes AVP/secretagogin dual-labeling. *Abbreviations:* lv, lateral ventricle; PVNm, magnocellular part of the paraventricular nucleus of the hypothalamus; scgn, secretagogin.

(**B$_3$**) Secretagogin$^+$ neurons had smaller somatic diameters than AVP$^+$ or oxytocin$^+$ neurons yet without a difference in their diameter quotient, a measure of ovoid profiles (**B$_4$**).

(**C-D$_3$**) Terminal-like profiles in the posterior pituitary suggesting that secretagogin can co-exist, even if infrequently with AVP. Solanum tuberosum lectin (Sol. Tub) was used to identify blood vessels. *Scale bars* = 100 µm (B), 10 µm (B$_1$,B$_2$), 2 µm (C-D$_3$).

Figure 2 Ultrastructural analysis suggests the prevalence of membrane-bound secretagogoin.

(**A**) Secretagogin (scgn) distribution at the ultrastructural level as revealed by pre-embedding silver-enhanced immunogold labeling. Secretagogin (*arrowheads*) was localized to membranous organelles in the perikarya (**A**), particularly the plasmalemma (**A$_1$**) and endoplasmic reticulum (ER) in neuronal somata (s; **A$_2$**). Open rectangle in "A" denotes the location of insets.

(**B**) Pre-embedding secretagogin labeling (*arrowheads*) was also seen in dendrite (d) segments.

(**C**) In axo-dendritic terminals (ax), secretagogin was closely associated with synaptic vesicles along the plasmalemma (*arrowheads*). Semi-transparent shading was used to visually dissociate subcellular compartments. *Scale bars* = 1 µm (A), 500 nm (B,C), 200 nm (A$_1$,A$_2$).

(**D**) Quantitative analysis of subcellular secretagogin distribution upon electron microscopy detection of silver-enhanced gold particles. Particles were considered as membrane bound when they were at <50 nm of a membrane (plasma membrane or endomembrane; i.e. secretory vesicle, Golgi or endoplasmic reticulum). In the soma of PVN neurons, significantly more particles were found in the cytosol as along the plasma membrane ($p < 0.01$). In contrast, membrane association predominated in axonal nerve endings in the median eminence ($p < 0.05$). Note that a significant proportion of particles was found adjacent to endomembranes in all subcellular compartments studied.

Figure 3 Electrophysiological classification of secretagogin$^+$ parvocellular neurons.

(**A-A$_3$**) Biocytin-filled neuron immunonegative for secretagogin yet containing AVP/oxytocin (a mixture of magnocellular markers was used in triple-labelling experiments).

(**B-B$_2$**) Secretagogin$^+$ biocytin-filled neuron lacking AVP/oxytocin immunosignal.

(**C,C$_1$**) Dendritic reconstruction of secretagogin$^-$ and secretagogin$^+$ neurons at their actual location in the paraventricular nucleus of the hypothalamus.

(**D**) Electrophysiological characteristics of magnocellular and parvocellular neurons. The waveform of repetitive action potential firing is shown on the left, while differential channel characteristics are depicted on the right. Examples of secretagogin$^+$ neurons are shown in red.

(**E**) Pie diagrams showing the grouping of PVN neurons in the PVN (*upper row*) and in adjacent pre-autonomic areas (*lower row*) cumulatively based on electrophysiological criteria listed in Table S1. Secretagogin$^+$ neurons typically belonged to *IIa* and *Ia* subtypes. *Scale bars* = 50 µm (A), 8 µm (A$_3$,B$_1$). *Abbreviations*: lv, lateral ventricle; PVN, paraventricular nucleus.

Figure 4 Molecular identity of secretagogin$^+$ paraventricular neurons.

Single-cell mRNA transcriptome profiling of dissociated cells from the mouse paraventricular nucleus. (**A**) Differential clustering based on secretagogin (Scgn), neuropeptide, hormone and hormone receptor mRNA expression. Secretagogin-expressing(+) neurons (*red arrows*) typically contained corticotropin releasing hormone (Crh) and Nr3c1 mRNA transcripts. (**A$_1$**) Clusters of gene transcripts from 130 cells reveal the phenotypic segregation of PVN neurons. Increasing mRNA copy numbers were depicted by a color gradient from deep blue (not detected) to red (high numbers). (**B**) Venn diagrams depicting the (non-)overlapping relationships of select mRNA transcripts used to molecularly define PVN neurons. (**B$_1$**) Cumulative ratio of phenotypic diversity amongst secretagogin$^+$ neurons. Note that Crh and/or GABA (derived from Gad1, Gad2 and Slc32a1 mRNA expression)

co-existed with secretagogin in parvocellular neurons. A complete list of mRNAs found in secretagogin+ neurons was reported in Table S3.

(**C,C$_1$**) Secretagogin co-localization with GFP in the PVN (*solid arrowheads*) of adult CRH-GFP (BAC) reporter mice (Alon et al, 2009). Open arrowhead pinpoints a single-labeled neuron.

(**D-E$_3$**) We found secretagogin (scgn) co-expressed with CRH both in neuronal somata (*solid arrowheads*; **D$_1$-D$_3$**) and axon terminal-like specializations (*arrowheads*; **E-E$_2$**) in the PVN. Likewise, secretagogin$^+$ neurons harbored, yet infrequently, tyrosine hydroxylase (TH; *solid arrowheads*; **F-F$_3$**), GABA (**G-G$_2$**), somatostatin (Sst; **H-H$_3$**) and galanin (**I-I$_2$**). Open rectangles denote the general location of insets. Open arrowheads indicate the lack of co-localization. *Scale bars* = 40 μm (D,F,H), 25 μm (C_1), 10 μm (D_3,F_3,G_3,H_3), 4 μm (E_3,I_3).

Figure 5 Secretagogin is a Ca^{2+} sensor protein.

(**A-A$_2$**) Secretagogin co-existed in the majority of CRH$^+$ nerve endings in the median eminence (ME). Open rectangle denotes the general location of "B,B_1".

(**B,B$_1$**) Large axon terminals in the median eminence were immunopositive for secretagogin with silver-intensified immunogold particles (*open arrowheads*) associated to axonal membrane and dense-core vesicles (see Fig. 1D for quantitative data). Solid arrowheads denote silver deposits particles proximal to the plasmalemma.

(**C**) Immunoprecipitation using an anti-secretagogin antibody in Ca^{2+}-free and Ca^{2+}-loaded conditions was subtractively used to decipher the Ca^{2+}-dependent protein interactions. Silver-stained gel is shown. (**C$_1$**) Ontology classification of the 99 protein hits based on primary function assignments. Unbiased MALDI-TOF proteomics was used to identify interacting proteins. The most abundant hits (Table S4 is referred to for details on individual proteins) are proteins implicated in vesicle fusion, trafficking, transport and formation and the regulation of vesicle exocytosis. "Other" refers to a group of proteins without known function.

(**D**) Single-cell transcriptomics was used to validate the above proteome data by clustering mRNA transcripts encoding proteins that underpin vesicular release processes (red color labels highest mRNA abundance whereas dark blue color indicates the lack of mRNA expression).

(**E-E$_3$**) Secretagogin$^+$ somata and terminals labeled for Sec22b (*arrowheads*), implicated in vesicle trafficking (Hay et al, 1997), in both the PVN and median eminence.

(**F-F$_3$**) Rab3, a family of vesicular fusion and transport proteins (Schluter et al, 2006), was found co-localized with secretagogin (*arrowheads*) in the median eminence. Neuronal somata in the PVN lacked appreciable co-localization. Note

that neither our MALDI-TOF analysis nor histochemical probing allowed the precise identification of individual Rab3C-E family members. *Scale bars* = 10 µm (A_1,E_3), 7 µm (E), 500 nm (B), 150 nm (B_1).

Figure 6 Secretagogin regulates CRH release *in vitro* and *in vivo*.

(**A,A$_1$**) siRNA-mediated secretagogin (scgn) knock-down in cultured hypothalamic neurons, as indicated by reduced secretagogin immunoreactivity (**A**), decreased CRH content in the culture medium (**A$_1$**).

(**B-B$_2$**) Transient overexpression of secretagogin in immortalized CRH-expressing mHypoE-44 hypothalamic cells significantly reduced CRH immunofluorescence intensity in secretagogin$^+$ cell bodies, indirectly supporting enhanced CRH release. All experiments were performed in triplicate.

(**C,C$_1$**) siRNA-mediated *in vivo* silencing of secretagogin mRNA expression in the PVN provoked somatic CRH accumulation (*arrowheads*). (**C$_2$**) Quantitative analysis demonstrating significantly increased somatic CRH contents. Note that somatic secretagogin levels remained unchanged, which we interpret as data on a neuronal contingent not affected by siRNA silencing. The lack of secretagogin/CRH co-localization suggests that secretagogin expression fell below detection threshold in many CRH$^+$ neurons.

(**D,D$_1$**) Individual data points show maximal CRH fluorescence intensity (grey scale arbitrary unit (a.u.) expression) in PVN neurons that have low or no secretagoogin expression after siRNA infusion.

Data in (**C$_2$**) were normalized to those in non-targeting siRNA controls. **p* < 0.05 *vs*. control. *Scale bars* = 150 µm (C,C_1), 50 nm (B,B_1).

Figure 7 Secretagogin$^+$ neurons gate the CRH-ACTH axis in response to acute stress.

(**A,A$_1$**) Paraventricular secretagogin-immunoreactive (scgn$^+$) neurons weakly expressed CRH (*open arrowheads*) but not c-fos under control conditions.

(**B,B$_1$**) Stress induced by subcutaneous injection of formalin triggered co-expression of c-fos and CRH in secretagogin$^+$ paraventricular neurons (*arrowheads*).

(**C,D**) *In vivo* siRNA-mediated silencing of secretagogin expression in the PVN occluded the stress-induced surge of serum ACTH levels, and significantly reduced the increase in plasma corticosterone (**D**). **p* < 0.05 *vs*. control. *Scale bars* = 300 µm (A,B), 25 µm (A_1,B_1).

REFERENCES

Aguilera G, Kiss A, Liu Y, and Kamitakahara A (2007) Negative regulation of corticotropin releasing factor expression and limitation of stress response. *Stress* **10:** 153-161

Alon T, Zhou L, Perez CA, Garfield AS, Friedman JM, and Heisler LK (2009) Transgenic mice expressing green fluorescent protein under the control of the corticotropin-releasing hormone promoter. *Endocrinology* **150:** 5626-5632

Alonso G, Szafarczyk A, and Assenmacher I (1986) Immunoreactivity of hypothalamo-neurohypophysial neurons which secrete corticotropin-releasing hormone (CRH) and vasopressin (Vp): immunocytochemical evidence for a correlation with their functional state in colchicine-treated rats. *Exp Brain Res* **61:** 497-505

Andressen C, Blumcke I, and Celio MR (1993) Calcium-binding proteins: selective markers of nerve cells. *Cell Tissue Res* **271:** 181-208

Arai R, Jacobowitz DM, and Deura S (1993) Immunohistochemical localization of calretinin-, calbindin-D28k- and parvalbumin-containing cells in the hypothalamic paraventricular and supraoptic nuclei of the rat. *Brain Res* **618:** 323-327

Armario A (2006) The hypothalamic-pituitary-adrenal axis: what can it tell us about stressors? *CNS Neurol Disord Drug Targets* **5:** 485-501

Bargmann W (1969) The neurosecretory diencephalon-hypophyseal system and its synaptic connections. *J Neurovisc Relat* **31:** Suppl-77

Barna I and Koenig JI (1992) Effects of mediobasal hypothalamic lesion on immunoreactive ACTH/beta-endorphin levels in cerebrospinal fluid, in discrete brain regions, in plasma, and in pituitary of the rat. *Brain Res* **593:** 69-76

Bauer MC, O'Connell DJ, Maj M, Wagner L, Cahill DJ, and Linse S (2011) Identification of a high-affinity network of secretagogin-binding proteins involved in vesicle secretion. *Mol Biosyst* **7:** 2196-2204

Baxter JD and Forsham PH (1972) Tissue effects of glucocorticoids. *Am J Med* **53:** 573-589

Birkenkamp-Demtroder K, Wagner L, Brandt SF, Bording AL, Gartner W, Scherubl H, Heine B, Christiansen P, and Orntoft TF (2005) Secretagogin is a novel marker for neuroendocrine differentiation. *Neuroendocrinology* **82:** 121-138

Brose N, Petrenko AG, Sudhof TC, and Jahn R (1992) Synaptotagmin: a calcium sensor on the synaptic vesicle surface. *Science* **256:** 1021-1025

Cam GR and Bassett JR (1983) The plasma levels of ACTH following exposure to stress or nicotine. *Arch Int Pharmacodyn Ther* **264:** 154-167

Carafoli E, Santella L, Branca D, and Brini M (2001) Generation, control, and processing of cellular calcium signals. *Crit Rev Biochem Mol Biol* **36:** 107-260

Cazalis M, Dayanithi G, and Nordmann JJ (1985) The role of patterned burst and interburst interval on the excitation-coupling mechanism in the isolated rat neural lobe. *J Physiol* **369:** 45-60

Ceccatelli S, Cintra A, Hokfelt T, Fuxe K, Wikstrom AC, and Gustafsson JA (1989) Coexistence of glucocorticoid receptor-like immunoreactivity with neuropeptides in the hypothalamic paraventricular nucleus. *Exp Brain Res* **78:** 33-42

Clapham DE (2007) Calcium signaling. *Cell* **131:** 1047-1058

Cortes R, Ceccatelli S, Schalling M, and Hokfelt T (1990) Differential effects of intracerebroventricular colchicine administration on the expression of mRNAs for neuropeptides and neurotransmitter enzymes, with special emphasis on galanin: an in situ hybridization study. *Synapse* **6:** 369-391

Dayanithi G, Forostyak O, Ueta Y, Verkhratsky A, and Toescu EC (2012) Segregation of calcium signalling mechanisms in magnocellular neurones and terminals. *Cell Calcium* **51:** 293-299

de Kloet ER, Joels M, and Holsboer F (2005) Stress and the brain: from adaptation to disease. *Nat Rev Neurosci* **6:** 463-475

Dierickx K and Vandesande F (1979) Immunocytochemical localization of somatostatin-containing neurons in the rat hypothalamus. *Cell Tissue Res* **201:** 349-359

Donner KM, Hiltunen TP, Janne OA, Sane T, and Kontula K (2013) Generalized glucocorticoid resistance caused by a novel two-nucleotide deletion in the hormone-binding domain of the glucocorticoid receptor gene NR3C1. *Eur J Endocrinol* **168:** K9-K18

Dutton A and Dyball RE (1979) Phasic firing enhances vasopressin release from the rat neurohypophysis. *J Physiol* **290:** 433-440

Everitt BJ, Meister B, Hokfelt T, Melander T, Terenius L, Rokaeus A, Theodorsson-Norheim E, Dockray G, Edwardson J, Cuello C, and . (1986) The hypothalamic arcuate nucleus-median eminence complex: immunohistochemistry of transmitters, peptides and DARPP-32 with special reference to coexistence in dopamine neurons. *Brain Res* **396:** 97-155

Fuxe K, Wikstrom AC, Okret S, Agnati LF, Harfstrand A, Yu ZY, Granholm L, Zoli M, Vale W, and Gustafsson JA (1985) Mapping of glucocorticoid receptor immunoreactive neurons in the rat tel- and diencephalon using a monoclonal antibody against rat liver glucocorticoid receptor. *Endocrinology* **117:** 1803-1812

Gainer H, Yamashita M, Fields RL, House SB, and Rusnak M (2002) The magnocellular neuronal phenotype: cell-specific gene expression in the hypothalamo-neurohypophysial system. *Prog Brain Res* **139:** 1-14

Guillemin R (1978) Peptides in the brain: the new endocrinology of the neuron. *Science* **202:** 390-402

Haam J, Popescu IR, Morton LA, Halmos KC, Teruyama R, Ueta Y, and Tasker JG (2012) GABA is excitatory in adult vasopressinergic neuroendocrine cells. *J Neurosci* **32:** 572-582

Hallbeck M, Blomqvist A, and Hermanson O (1996) Ca2+/calmodulin-dependent kinase II immunoreactivity in the rat hypothalamus. *Neuroreport* **7:** 1957-1960

Harris GW (1972) Humours and hormones. *J Endocrinol* **53:** 2-23

Hata Y, Slaughter CA, and Sudhof TC (1993) Synaptic vesicle fusion complex contains unc-18 homologue bound to syntaxin. *Nature* **366:** 347-351

Hay JC, Chao DS, Kuo CS, and Scheller RH (1997) Protein interactions regulating vesicle transport between the endoplasmic reticulum and Golgi apparatus in mammalian cells. *Cell* **89:** 149-158

Herman JP, Schafer MK, Thompson RC, and Watson SJ (1992) Rapid regulation of corticotropin-releasing hormone gene transcription in vivo. *Mol Endocrinol* **6:** 1061-1069

Hirokawa N and Takemura R (2005) Molecular motors and mechanisms of directional transport in neurons. *Nat Rev Neurosci* **6:** 201-214

Horvath TL and Gao XB (2005) Input organization and plasticity of hypocretin neurons: possible clues to obesity's association with insomnia. *Cell Metab* **1:** 279-286

Hrabovszky E, Wittmann G, Turi GF, Liposits Z, and Fekete C (2005) Hypophysiotropic thyrotropin-releasing hormone and corticotropin-releasing hormone neurons of the rat contain vesicular glutamate transporter-2. *Endocrinology* **146:** 341-347

Islam S, Kjallquist U, Moliner A, Zajac P, Fan JB, Lonnerberg P, and Linnarsson S (2011) Characterization of the single-cell transcriptional landscape by highly multiplex RNA-seq. *Genome Res* **21:** 1160-1167

Islam S, Zeisel A, Joost S, La MG, Zajac P, Kasper M, Lonnerberg P, and Linnarsson S (2014) Quantitative single-cell RNA-seq with unique molecular identifiers. *Nat Methods* **11:** 163-166

Keegan CE, Herman JP, Karolyi IJ, O'Shea KS, Camper SA, and Seasholtz AF (1994) Differential expression of corticotropin-releasing hormone in developing mouse embryos and adult brain. *Endocrinology* **134:** 2547-2555

Keimpema E, Barabas K, Morozov YM, Tortoriello G, Torii M, Cameron G, Yanagawa Y, Watanabe M, Mackie K, and Harkany T (2010) Differential subcellular recruitment of monoacylglycerol lipase generates spatial specificity of 2-arachidonoyl glycerol signaling during axonal pathfinding. *J Neurosci* **30:** 13992-14007

Kiss A, Palkovits M, and Aguilera G (1996) Neural regulation of corticotropin releasing hormone (CRH) and CRH receptor mRNA in the hypothalamic paraventricular nucleus in the rat. *J Neuroendocrinol* **8:** 103-112

Kiss JZ, Cassell MD, and Palkovits M (1984) Analysis of the ACTH/beta-End/alpha-MSH-immunoreactive afferent input to the hypothalamic paraventricular nucleus of rat. *Brain Res* **324:** 91-99

Kiss JZ, Martos J, and Palkovits M (1991) Hypothalamic paraventricular nucleus: a quantitative analysis of cytoarchitectonic subdivisions in the rat. *J Comp Neurol* **313:** 563-573

Kiss JZ, Palkovits M, Zaborszky L, Tribollet E, Szabo D, and Makara GB (1983) Quantitative histological studies on the hypothalamic paraventricular nucleus in rats: I. Number of cells and synaptic boutons. *Brain Res* **262:** 217-224

Kita T, Chihara K, Abe H, Minamitani N, Kaji H, Kodama H, Chiba T, Fujita T, and Yanaihara N (1986) Regional distribution of gastrin-releasing peptide- and somatostatin-like immunoreactivity in the rabbit hypothalamus. *Brain Res* **398:** 18-22

Kodama T, Guerrero S, Shin M, Moghadam S, Faulstich M, and du LS (2012) Neuronal classification and marker gene identification via single-cell expression profiling of brainstem vestibular neurons subserving cerebellar learning. *J Neurosci* **32:** 7819-7831

Korte SM (2001) Corticosteroids in relation to fear, anxiety and psychopathology. *Neurosci Biobehav Rev* **25:** 117-142

Kovacs KJ and Sawchenko PE (1996) Sequence of stress-induced alterations in indices of synaptic and transcriptional activation in parvocellular neurosecretory neurons. *J Neurosci* **16:** 262-273

Lee S, Han TH, Sonner PM, Stern JE, Ryu PD, and Lee SY (2008) Molecular characterization of T-type Ca(2+) channels responsible for low threshold spikes in hypothalamic paraventricular nucleus neurons. *Neuroscience* **155:** 1195-1203

Lee SK, Lee S, Shin SY, Ryu PD, and Lee SY (2012) Single cell analysis of voltage-gated potassium channels that determines neuronal types of rat hypothalamic paraventricular nucleus neurons. *Neuroscience* **205:** 49-62

Linden M, Lind SB, Mayrhofer C, Segersten U, Wester K, Lyutvinskiy Y, Zubarev R, Malmstrom PU, and Pettersson U (2012) Proteomic analysis of urinary biomarker candidates for nonmuscle invasive bladder cancer. *Proteomics* **12:** 135-144

Lovatt D, Ruble BK, Lee J, Dueck H, Kim TK, Fisher S, Francis C, Spaethling JM, Wolf JA, Grady MS, Ulyanova AV, Yeldell SB, Griepenburg JC, Buckley PT, Kim J, Sul JY, Dmochowski IJ, and Eberwine J (2014) Transcriptome in vivo analysis (TIVA) of spatially defined single cells in live tissue. *Nat Methods* **11:** 190-196

Luther JA, Daftary SS, Boudaba C, Gould GC, Halmos KC, and Tasker JG (2002) Neurosecretory and non-neurosecretory parvocellular neurones of the hypothalamic paraventricular nucleus express distinct electrophysiological properties. *J Neuroendocrinol* **14:** 929-932

Luther JA and Tasker JG (2000) Voltage-gated currents distinguish parvocellular from magnocellular neurones in the rat hypothalamic paraventricular nucleus. *J Physiol* **523 Pt 1:** 193-209

Maejima Y, Sedbazar U, Suyama S, Kohno D, Onaka T, Takano E, Yoshida N, Koike M, Uchiyama Y, Fujiwara K, Yashiro T, Horvath TL, Dietrich MO, Tanaka S, Dezaki K, Oh I, Hashimoto K, Shimizu H, Nakata M, Mori M, and Yada T (2009) Nesfatin-1-regulated oxytocinergic signaling in the paraventricular nucleus causes anorexia through a leptin-independent melanocortin pathway. *Cell Metab* **10:** 355-365

Maj M, Milenkovic I, Bauer J, Berggard T, Veit M, Ilhan-Mutlu A, Wagner L, and Tretter V (2012) Novel insights into the distribution and functional aspects of the calcium binding protein secretagogin from studies on rat brain and primary neuronal cell culture. *Front Mol Neurosci* **5:** 84

Makara GB, Stark E, Karteszi M, Palkovits M, and Rappay G (1981) Effects of paraventricular lesions on stimulated ACTH release and CRF in stalk-median eminence of the rat. *Am J Physiol* **240:** E441-E446

Makino S, Hashimoto K, and Gold PW (2002) Multiple feedback mechanisms activating corticotropin-releasing hormone system in the brain during stress. *Pharmacol Biochem Behav* **73:** 147-158

McEwen BS (2007) Physiology and neurobiology of stress and adaptation: central role of the brain. *Physiol Rev* **87:** 873-904

Meister B, Hokfelt T, Geffard M, and Oertel W (1988) Glutamic acid decarboxylase- and gamma-aminobutyric acid-like immunoreactivities in corticotropin-releasing factor-containing parvocellular neurons of the hypothalamic paraventricular nucleus. *Neuroendocrinology* **48:** 516-526

Meister B, Villar MJ, Ceccatelli S, and Hokfelt T (1990) Localization of chemical messengers in magnocellular neurons of the hypothalamic supraoptic and paraventricular nuclei: an immunohistochemical study using experimental manipulations. *Neuroscience* **37:** 603-633

Mulder J, Zilberter M, Spence L, Tortoriello G, Uhlen M, Yanagawa Y, Aujard F, Hokfelt T, and Harkany T (2009) Secretagogin is a Ca2+-binding protein specifying subpopulations of telencephalic neurons. *Proc Natl Acad Sci U S A* **106:** 22492-22497

Naveilhan P, Hassani H, Lucas G, Blakeman KH, Hao JX, Xu XJ, Wiesenfeld-Hallin Z, Thoren P, and Ernfors P (2001) Reduced antinociception and plasma extravasation in mice lacking a neuropeptide Y receptor. *Nature* **409:** 513-517

Ohtori S, Takahashi K, Chiba T, Takahashi Y, Yamagata M, Sameda H, and Moriya H (2000) Fos expression in the rat brain and spinal cord evoked by noxious stimulation to low back muscle and skin. *Spine (Phila Pa 1976)* **25:** 2425-2430

Pacak K, Palkovits M, Kvetnansky R, Yadid G, Kopin IJ, and Goldstein DS (1995) Effects of various stressors on in vivo norepinephrine release in the hypothalamic paraventricular nucleus and on the pituitary-adrenocortical axis. *Ann N Y Acad Sci* **771:** 115-130

Palkovits M (1984) Neuropeptides in the hypothalamo-hypophyseal system: lateral retrochiasmatic area as a common gate for neuronal fibers towards the median eminence. *Peptides* **5 Suppl 1:** 35-39

Palkovits M (1987) Anatomy of neural pathways affecting CRH secretion. *Ann N Y Acad Sci* **512:** 139-148

Pang ZP and Sudhof TC (2010) Cell biology of Ca2+-triggered exocytosis. *Curr Opin Cell Biol* **22:** 496-505

Paxinos G and Franklin KBJ (2001). *The mouse brain in stereotaxic coordinates*. Academic Press, San Diego.

Pelletier G (1991) Anatomy of the hypothalamic-pituitary axis. *Methods Achiev Exp Pathol* **14:** 1-22

Petersen OH, Michalak M, and Verkhratsky A (2005) Calcium signalling: past, present and future. *Cell Calcium* **38:** 161-169

Pinto S, Roseberry AG, Liu H, Diano S, Shanabrough M, Cai X, Friedman JM, and Horvath TL (2004) Rapid rewiring of arcuate nucleus feeding circuits by leptin. *Science* **304:** 110-115

Rivier C and Vale W (1983) Influence of the frequency of ovine corticotropin-releasing factor administration on adrenocorticotropin and corticosterone secretion in the rat. *Endocrinology* **113:** 1422-1426

Rogstam A, Linse S, Lindqvist A, James P, Wagner L, and Berggard T (2007) Binding of calcium ions and SNAP-25 to the hexa EF-hand protein secretagogin. *Biochem J* **401:** 353-363

Sanchez F, Alonso JR, Arevalo R, Carretero J, Vazquez R, and Aijon J (1992) Calbindin D-28K- and parvalbumin-reacting neurons in the hypothalamic magnocellular neurosecretory nuclei of the rat. *Brain Res Bull* **28:** 39-46

Sapolsky RM, Krey LC, and McEwen BS (1986) The neuroendocrinology of stress and aging: the glucocorticoid cascade hypothesis. *Endocr Rev* **7:** 284-301

Sawchenko PE, Imaki T, Potter E, Kovacs K, Imaki J, and Vale W (1993) The functional neuroanatomy of corticotropin-releasing factor. *Ciba Found Symp* **172:** 5-21

Schally AV (1978) Aspects of hypothalamic regulation of the pituitary gland. *Science* **202:** 18-28

Schluter OM, Basu J, Sudhof TC, and Rosenmund C (2006) Rab3 superprimes synaptic vesicles for release: implications for short-term synaptic plasticity. *J Neurosci* **26:** 1239-1246

Schwaller B (2009) The continuing disappearance of "pure" Ca2+ buffers. *Cell Mol Life Sci* **66:** 275-300

Selye H and Fortier C (1949) Adaptive reactions to stress. *Res Publ Assoc Res Nerv Ment Dis* **29:** 3-18

Shapiro E, Biezuner T, and Linnarsson S (2013) Single-cell sequencing-based technologies will revolutionize whole-organism science. *Nat Rev Genet* **14:** 618-630

Shi TJ, Xiang Q, Zhang MD, Tortoriello G, Hammarberg H, Mulder J, Fried K, Wagner L, Josephson A, Uhlen M, Harkany T, and Hokfelt T (2012) Secretagogin is expressed in sensory CGRP neurons and in spinal cord of mouse and complements other calcium-binding proteins, with a note on rat and human. *Mol Pain* **8:** 80

Simmons DM and Swanson LW (2009) Comparison of the spatial distribution of seven types of neuroendocrine neurons in the rat paraventricular nucleus: toward a global 3D model. *J Comp Neurol* **516:** 423-441

Sollner T, Whiteheart SW, Brunner M, Erdjument-Bromage H, Geromanos S, Tempst P, and Rothman JE (1993) SNAP receptors implicated in vesicle targeting and fusion. *Nature* **362:** 318-324

Spiess J, Rivier J, Rivier C, and Vale W (1981) Primary structure of corticotropin-releasing factor from ovine hypothalamus. *Proc Natl Acad Sci U S A* **78:** 6517-6521

Stern JE (2001) Electrophysiological and morphological properties of pre-autonomic neurones in the rat hypothalamic paraventricular nucleus. *J Physiol* **537:** 161-177

Sudhof TC (2004) The synaptic vesicle cycle. *Annu Rev Neurosci* **27:** 509-547

Sudhof TC and Rothman JE (2009) Membrane fusion: grappling with SNARE and SM proteins. *Science* **323:** 474-477

Sutton RB, Fasshauer D, Jahn R, and Brunger AT (1998) Crystal structure of a SNARE complex involved in synaptic exocytosis at 2.4 A resolution. *Nature* **395:** 347-353

Swanson LW (1991) Biochemical switching in hypothalamic circuits mediating responses to stress. *Prog Brain Res* **87:** 181-200

Swanson LW and Sawchenko PE (1980) Paraventricular nucleus: a site for the integration of neuroendocrine and autonomic mechanisms. *Neuroendocrinology* **31:** 410-417

Swanson LW and Sawchenko PE (1983) Hypothalamic integration: organization of the paraventricular and supraoptic nuclei. *Annu Rev Neurosci* **6:** 269-324

Swanson LW, Sawchenko PE, and Lind RW (1986) Regulation of multiple peptides in CRF parvocellular neurosecretory neurons: implications for the stress response. *Prog Brain Res* **68:** 169-190

Swanson LW and Simmons DM (1989) Differential steroid hormone and neural influences on peptide mRNA levels in CRH cells of the paraventricular nucleus: a hybridization histochemical study in the rat. *J Comp Neurol* **285:** 413-435

Takamori S, Holt M, Stenius K, Lemke EA, Gronborg M, Riedel D, Urlaub H, Schenck S, Brugger B, Ringler P, Muller SA, Rammner B, Grater F, Hub JS, De Groot BL, Mieskes G, Moriyama Y, Klingauf J, Grubmuller H, Heuser J, Wieland F, and Jahn R (2006) Molecular anatomy of a trafficking organelle. *Cell* **127:** 831-846

Tang F, Barbacioru C, Wang Y, Nordman E, Lee C, Xu N, Wang X, Bodeau J, Tuch BB, Siddiqui A, Lao K, and Surani MA (2009) mRNA-Seq whole-transcriptome analysis of a single cell. *Nat Methods* **6:** 377-382

Tasker JG and Herman JP (2011) Mechanisms of rapid glucocorticoid feedback inhibition of the hypothalamic-pituitary-adrenal axis. *Stress* **14:** 398-406

Tobin V, Leng G, and Ludwig M (2012a) The involvement of actin, calcium channels and exocytosis proteins in somato-dendritic oxytocin and vasopressin release. *Front Physiol* **3:** 261

Tobin V, Schwab Y, Lelos N, Onaka T, Pittman QJ, and Ludwig M (2012b) Expression of exocytosis proteins in rat supraoptic nucleus neurones. *J Neuroendocrinol* **24:** 629-641

Tortoriello G, Morris CV, Alpar A, Fuzik J, Shirran SL, Calvigioni D, Keimpema E, Botting CH, Reinecke K, Herdegen T, Courtney M, Hurd YL, and Harkany T (2014) Miswiring the brain: Delta9-tetrahydrocannabinol disrupts cortical development by inducing an SCG10/stathmin-2 degradation pathway. *EMBO J* **33:** 668-685

Tsafrir D, Tsafrir I, Ein-Dor L, Zuk O, Notterman DA, and Domany E (2005) Sorting points into neighborhoods (SPIN): data analysis and visualization by ordering distance matrices. *Bioinformatics* **21:** 2301-2308

Vale W, Spiess J, Rivier C, and Rivier J (1981) Characterization of a 41-residue ovine hypothalamic peptide that stimulates secretion of corticotropin and beta-endorphin. *Science* **213:** 1394-1397

van Rossum EF, Voorhoeve PG, te Velde SJ, Koper JW, Delemarre-van de Waal HA, Kemper HC, and Lamberts SW (2004) The ER22/23EK polymorphism in the glucocorticoid receptor gene is associated with a beneficial body composition and muscle strength in young adults. *J Clin Endocrinol Metab* **89:** 4004-4009

Vogt MC, Paeger L, Hess S, Steculorum SM, Awazawa M, Hampel B, Neupert S, Nicholls HT, Mauer J, Hausen AC, Predel R, Kloppenburg P, Horvath TL, and Bruning JC (2014) Neonatal insulin action impairs hypothalamic neurocircuit formation in response to maternal high-fat feeding. *Cell* **156:** 495-509

Wagner L, Oliyarnyk O, Gartner W, Nowotny P, Groeger M, Kaserer K, Waldhausl W, and Pasternack MS (2000) Cloning and expression of secretagogin, a novel neuroendocrine- and pancreatic islet of Langerhans-specific Ca2+-binding protein. *J Biol Chem* **275:** 24740-24751

Wamsteeker Cusulin JI, Fuzesi T, Watts AG, and Bains JS (2013) Characterization of corticotropin-releasing hormone neurons in the paraventricular nucleus of the hypothalamus of Crh-IRES-Cre mutant mice. *PLoS One* **8:** e64943

Wickner W and Schekman R (2008) Membrane fusion. *Nat Struct Mol Biol* **15:** 658-664

Wynn PC, Aguilera G, Morell J, and Catt KJ (1983) Properties and regulation of high-affinity pituitary receptors for corticotropin-releasing factor. *Biochem Biophys Res Commun* **110:** 602-608

Yamamori E, Asai M, Yoshida M, Takano K, Itoi K, Oiso Y, and Iwasaki Y (2004) Calcium/calmodulin kinase IV pathway is involved in the transcriptional regulation of the corticotropin-releasing hormone gene promoter in neuronal cells. *J Mol Endocrinol* **33:** 639-649

Romanov, Alpar *et al*. - Figure 1R1
EMBOJ-2014-88977 (single column)

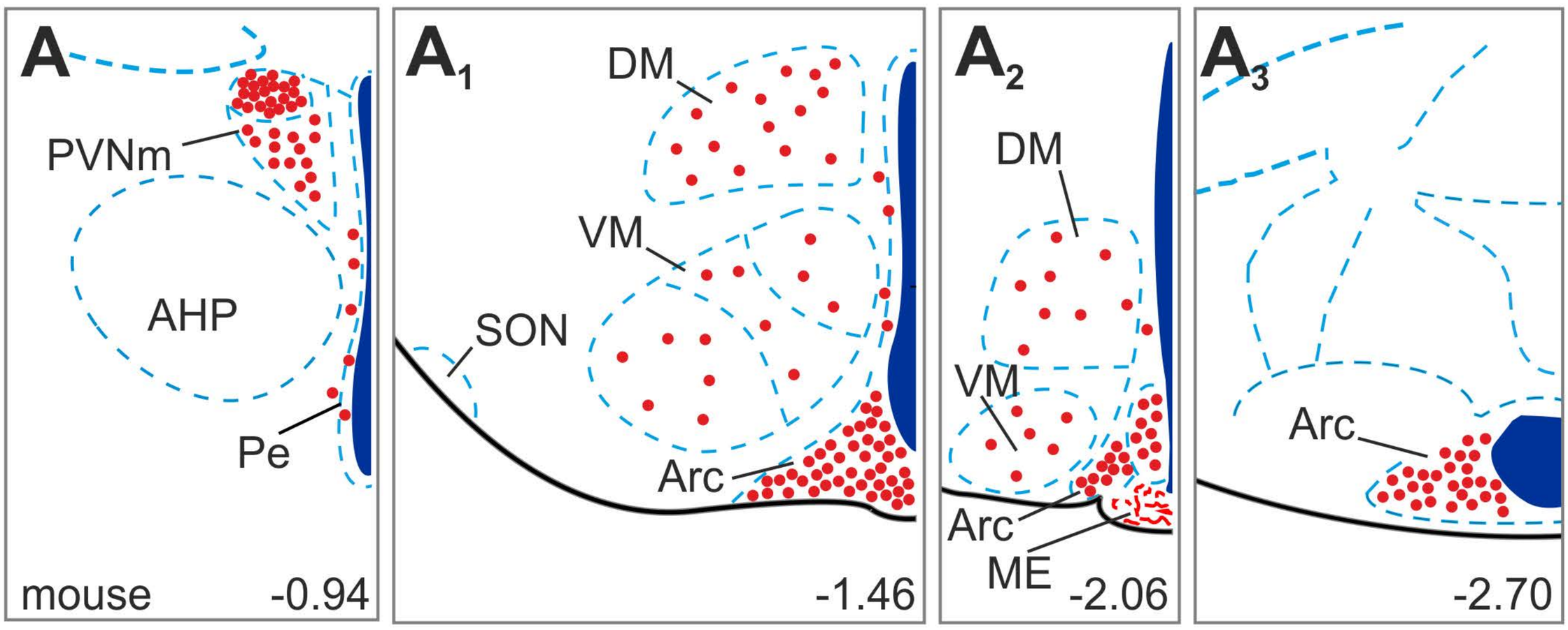

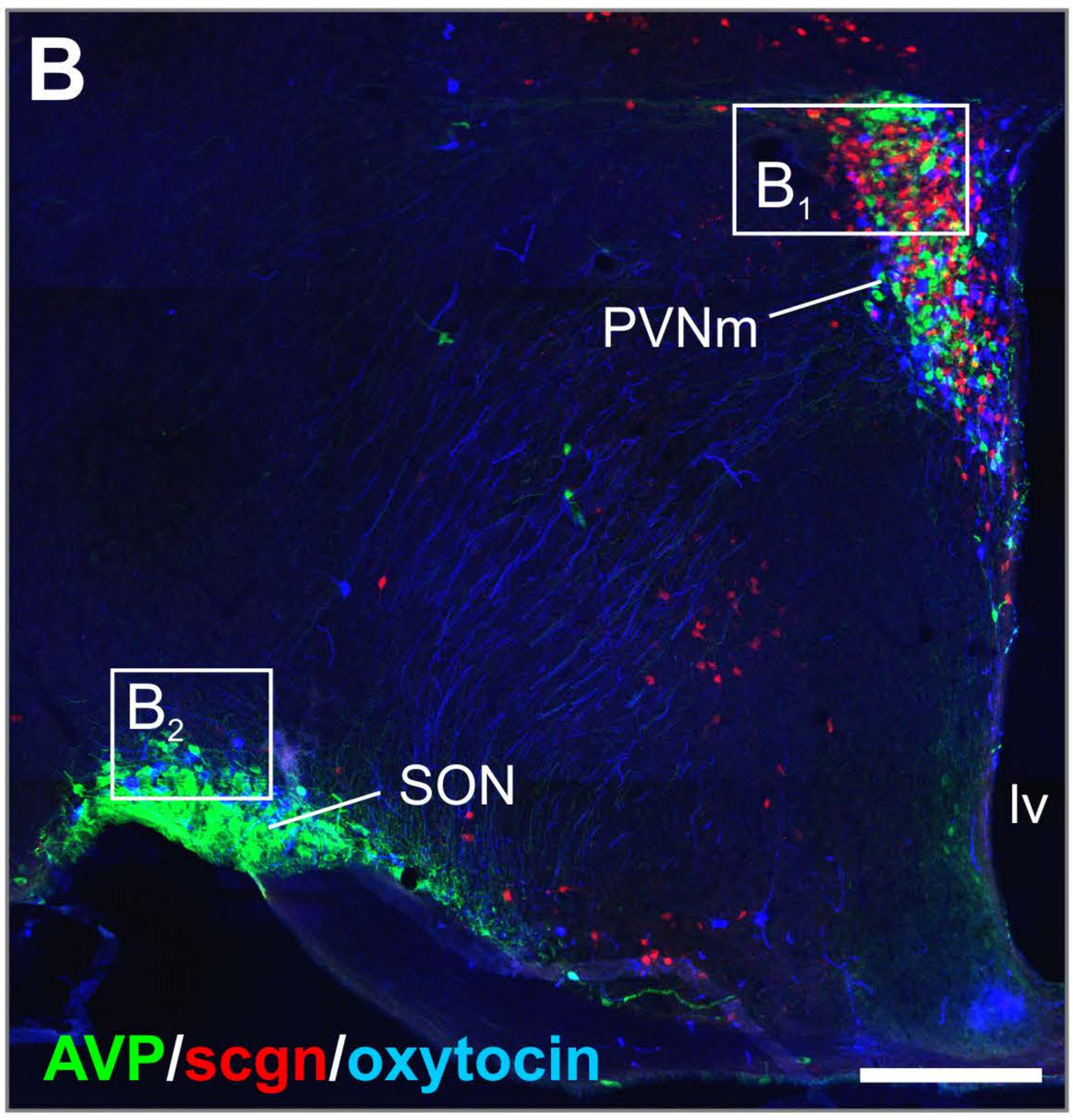

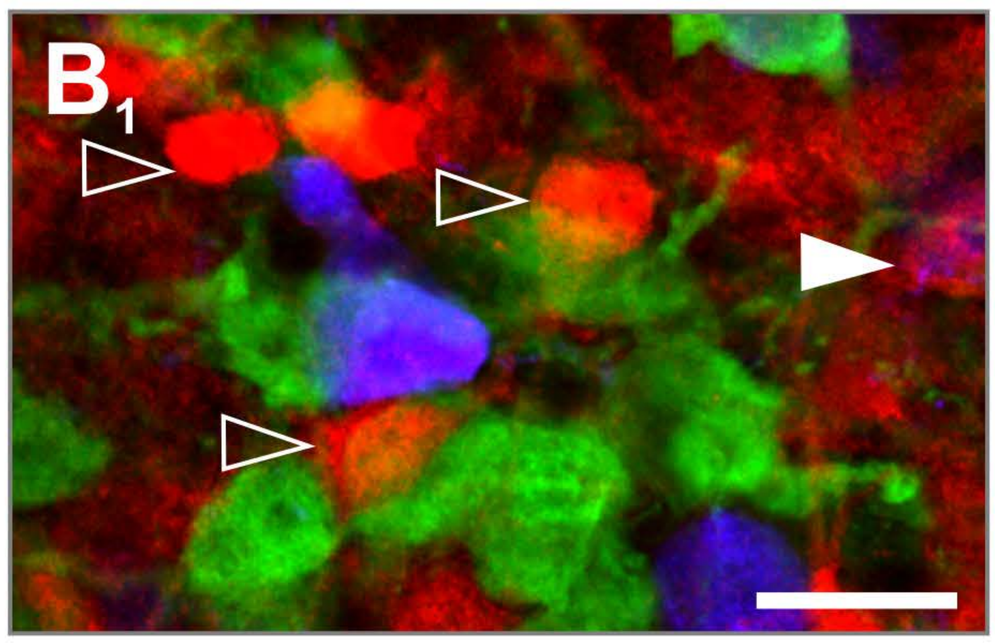

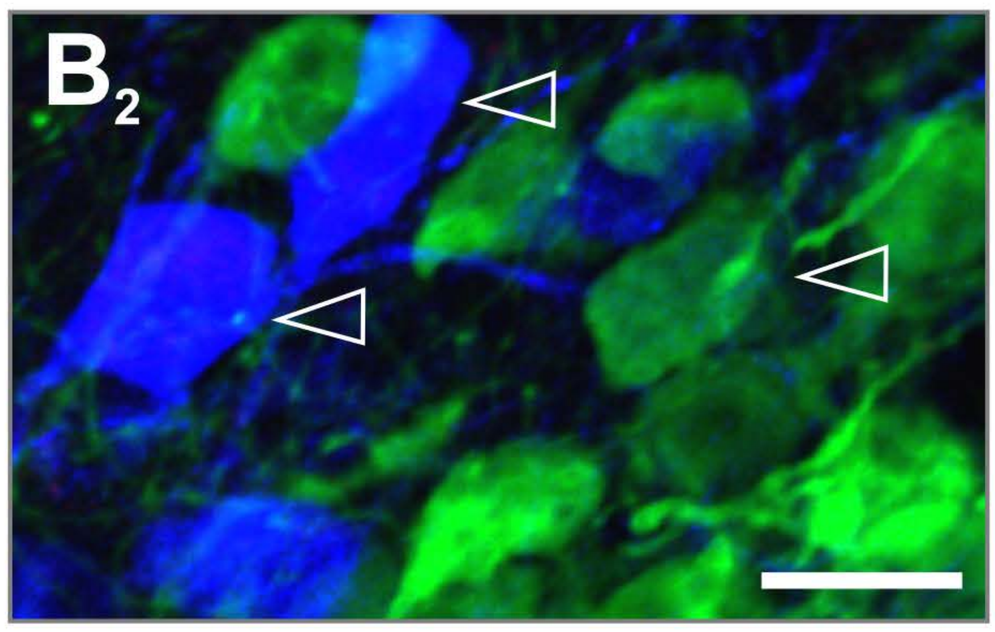

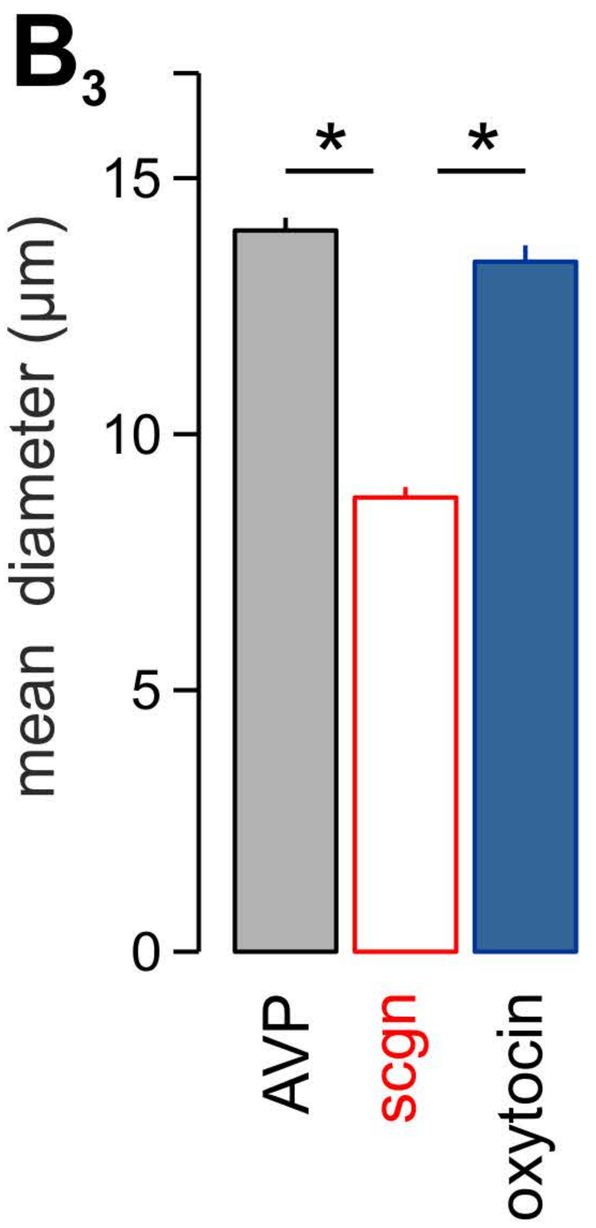

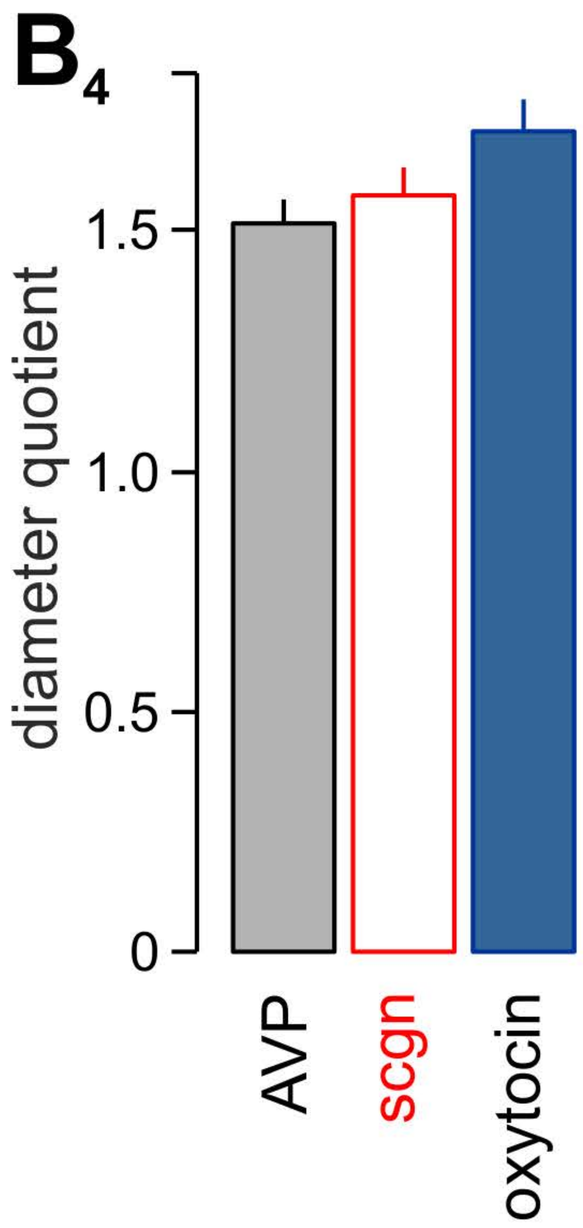

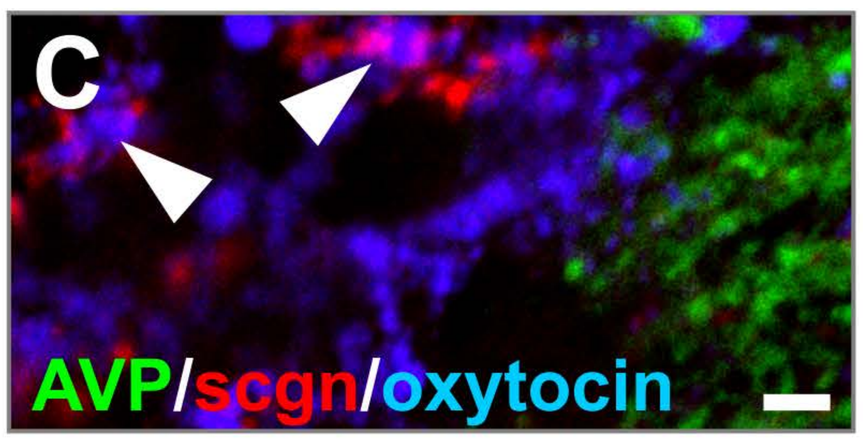

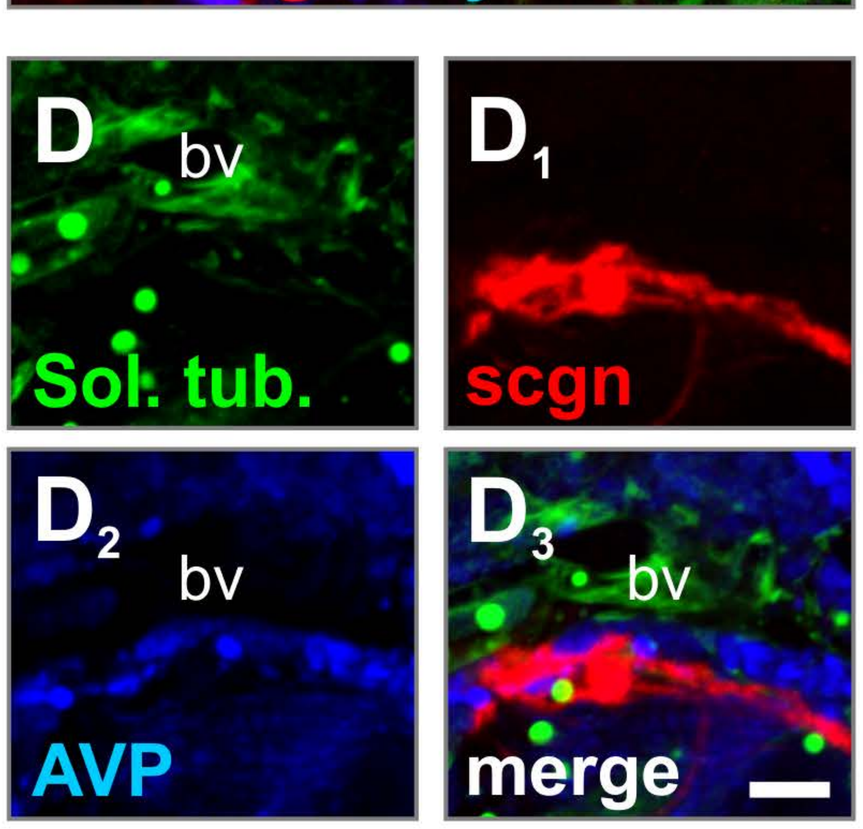

Romanov, Alpar *et al*. - Figure 2R1
EMBOJ-2014-88977 (1.5 columns)

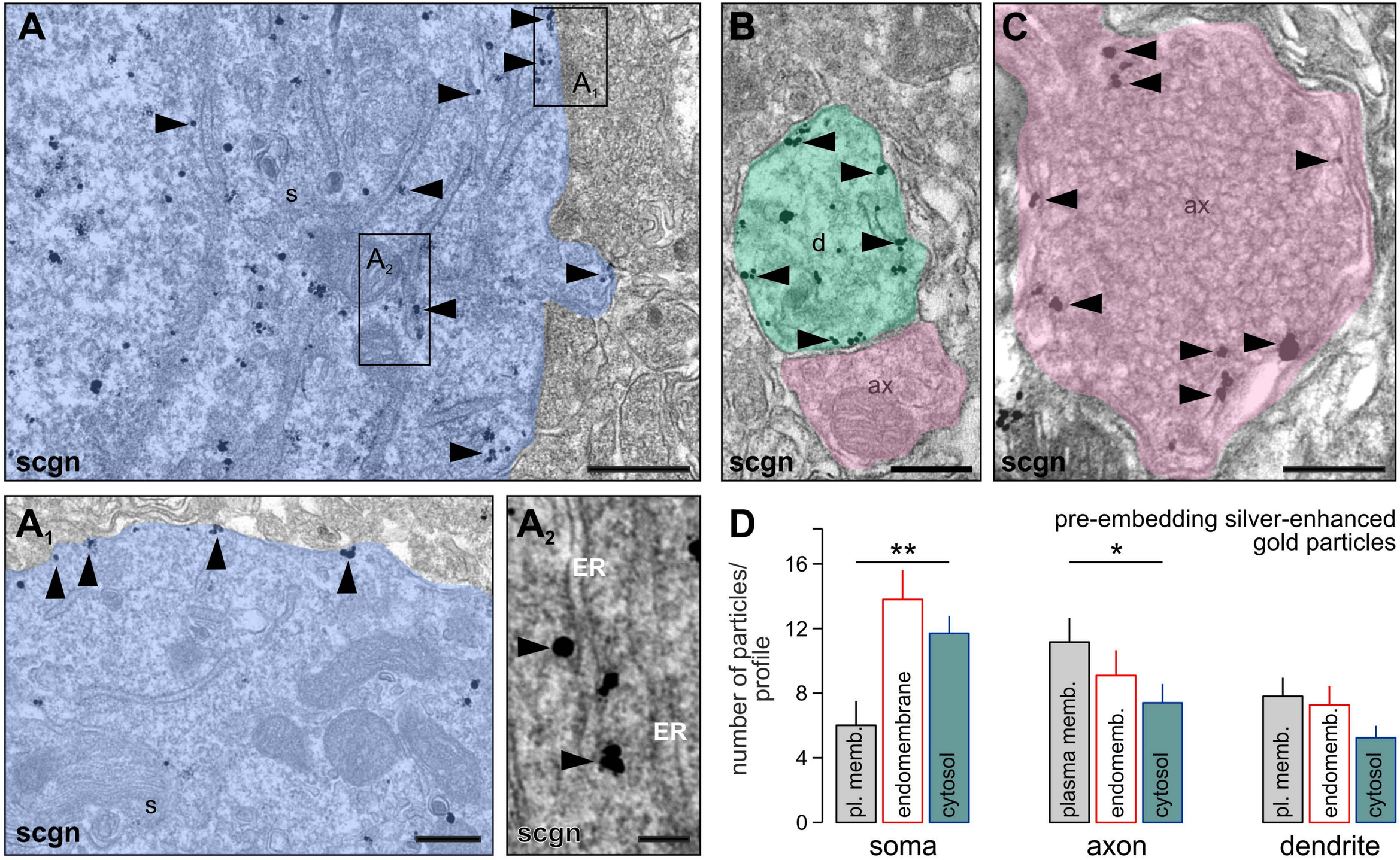

Romanov, Alpar *et al*. - Figure 3R1 EMBOJ-2014-88977 (1.5 columns)

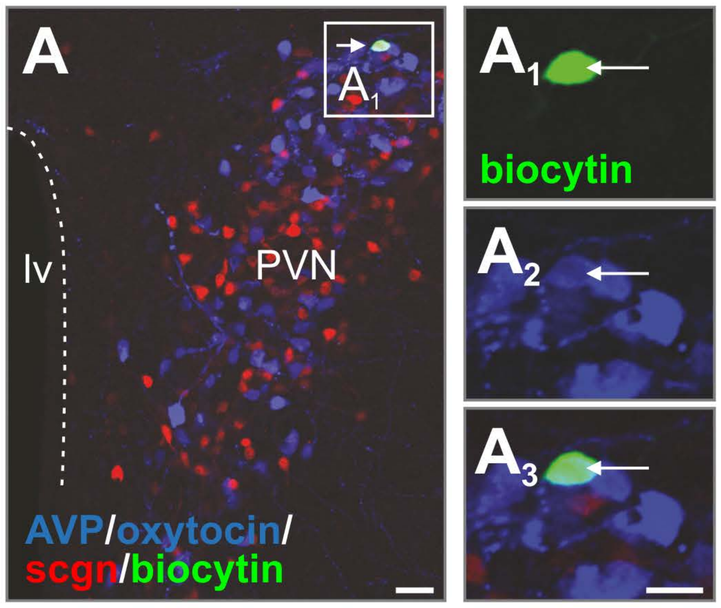

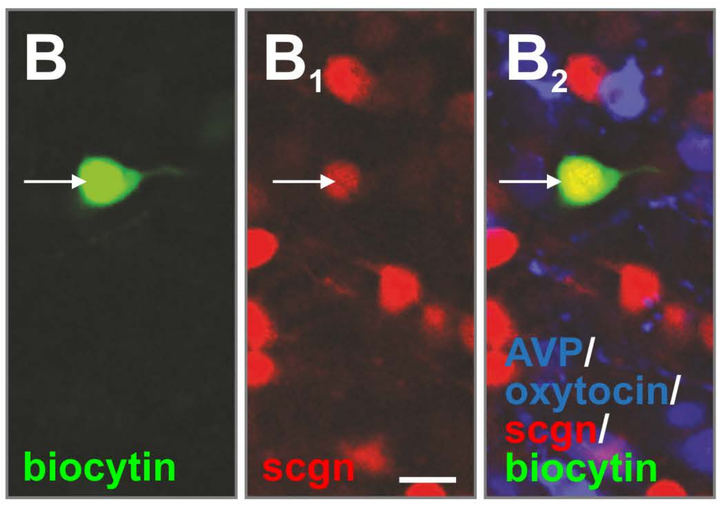

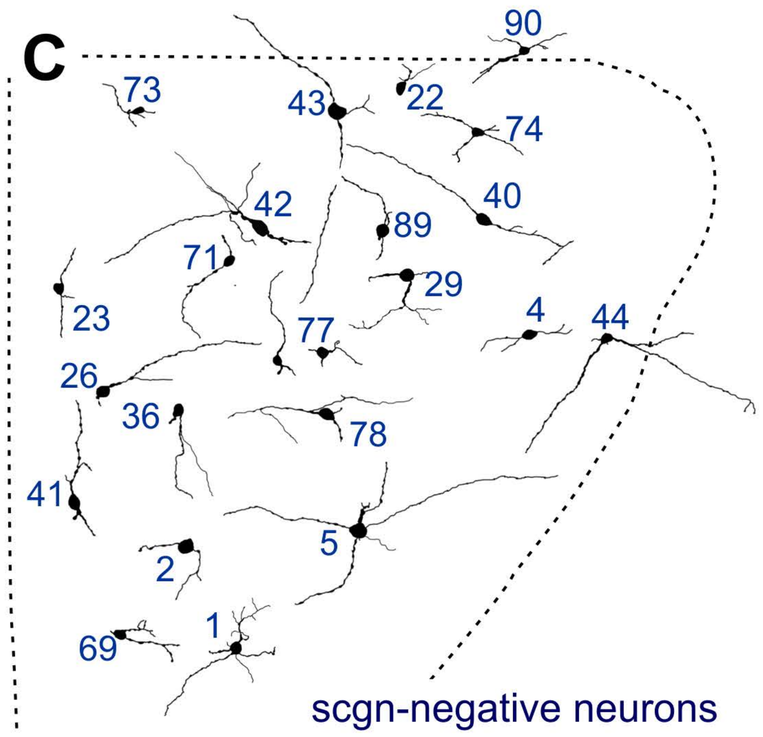

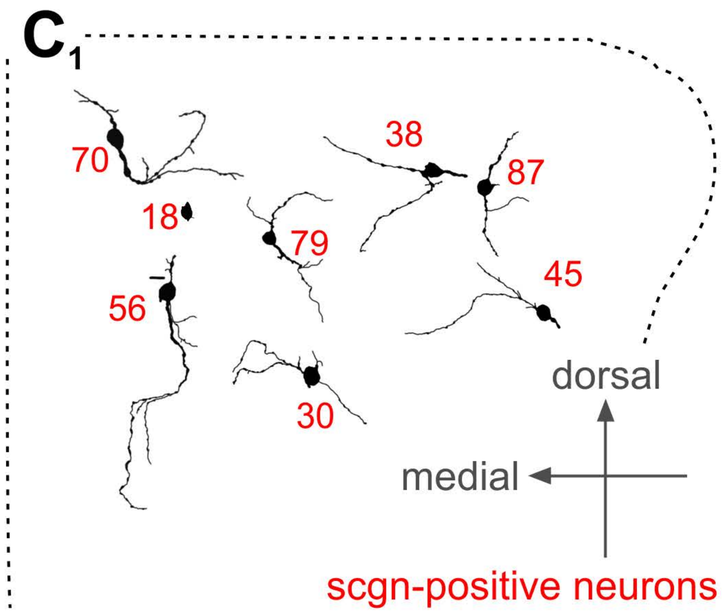

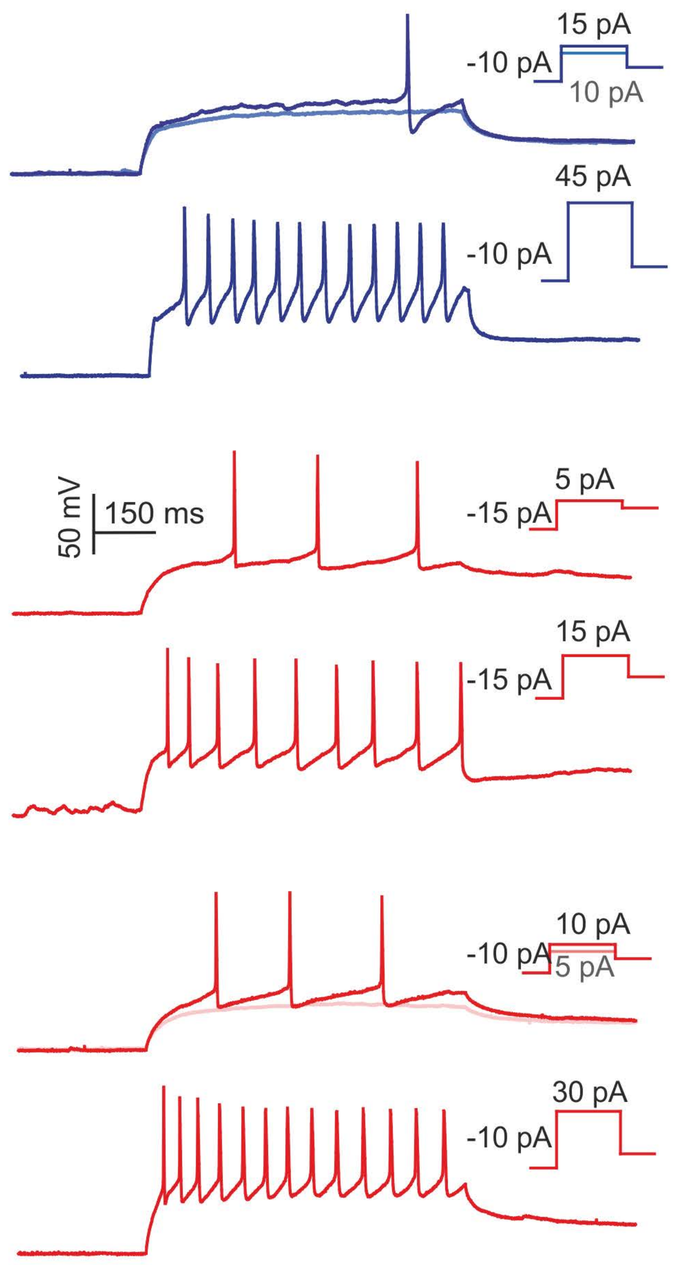

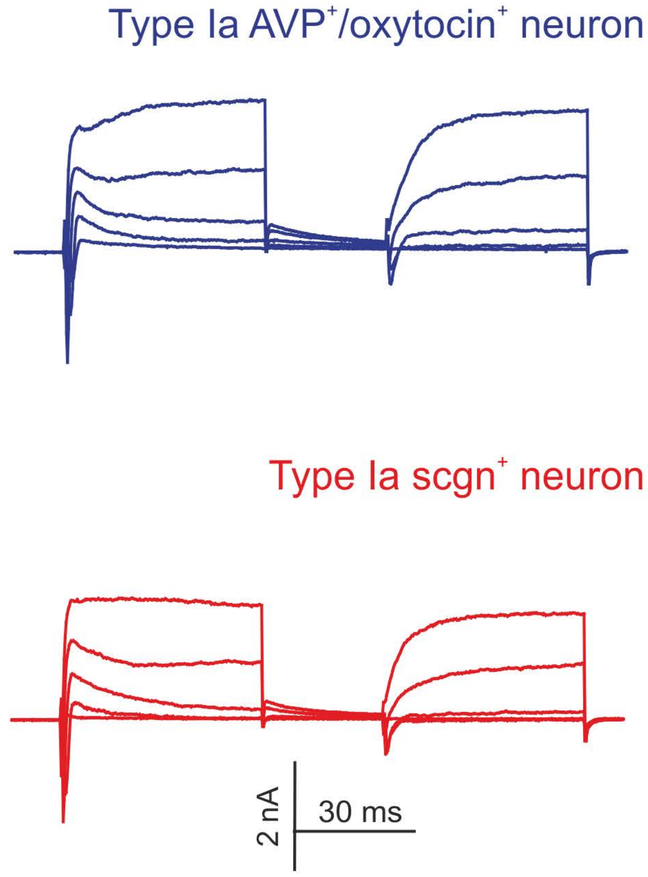

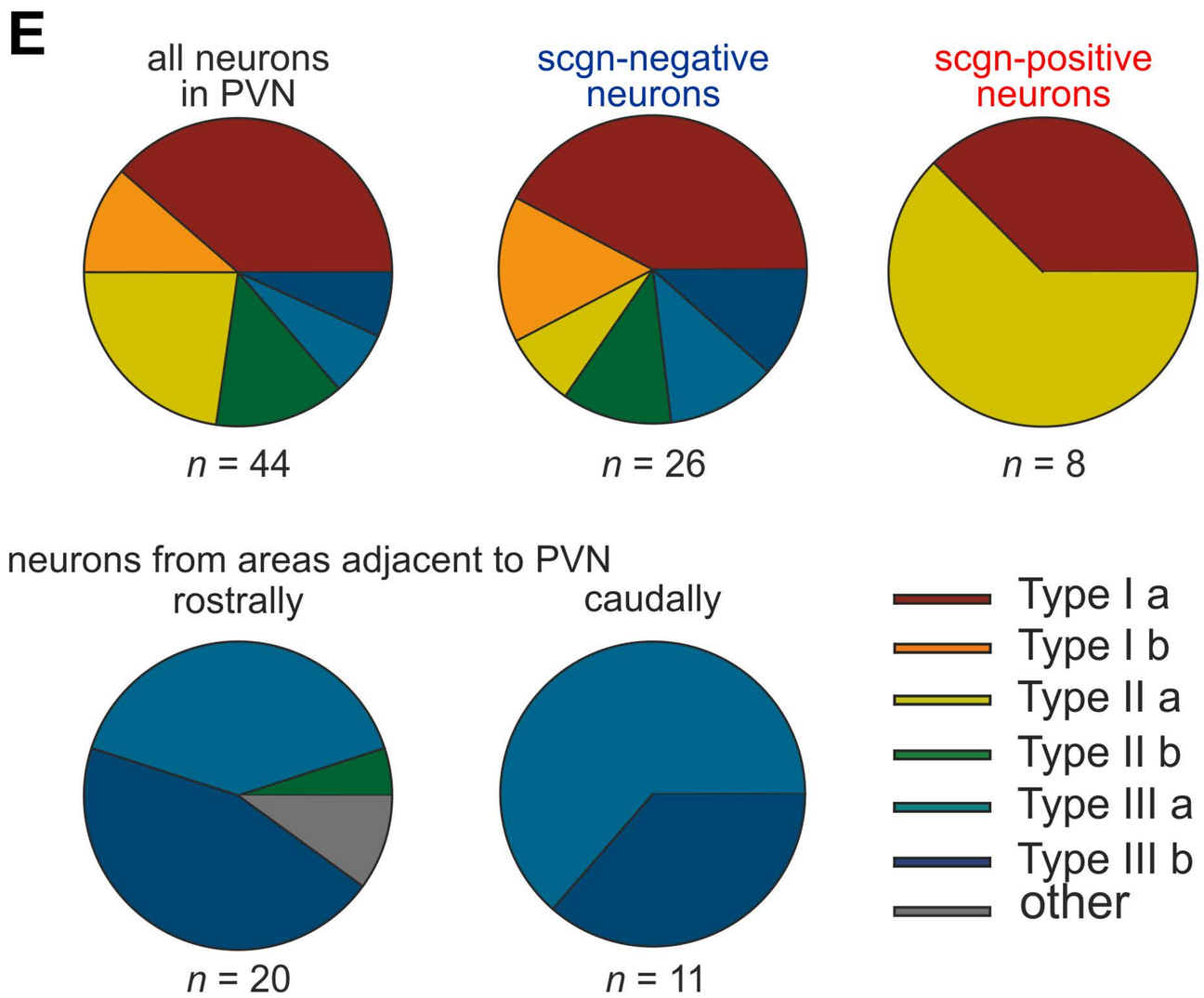

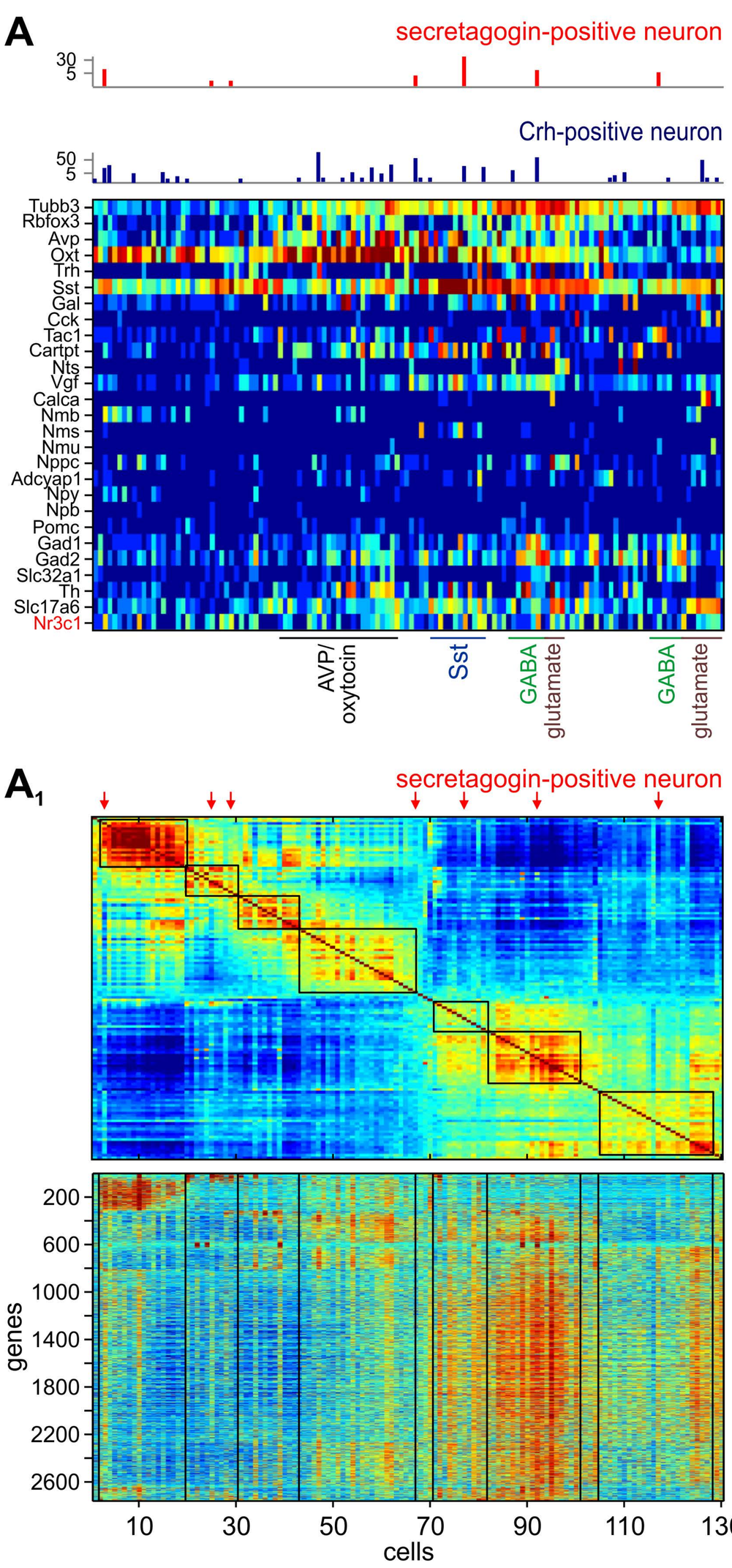
A
secretagogin-positive neuron
30
5
Crh-positive neuron
50
5
Tubb3
Rbfox3
Avp
Oxt
Trh
Sst
Gal
Cck
Tac1
Cartpt
Nts
Vgf
Calca
Nmb
Nms
Nmu
Nppc
Adcyap1
Npy
Npb
Pomc
Gad1
Gad2
Slc32a1
Th
Slc17a6
Nr3c1
AVP/ oxytocin
Sst
GABA glutamate
GABA glutamate
A1
secretagogin-positive neuron
200
600
1000
1400
1800
2200
2600
genes
10
30
50
70
90
110
130
cells
B
Trh
Tac1
Crh
Avp
Scgn
Oxytocin

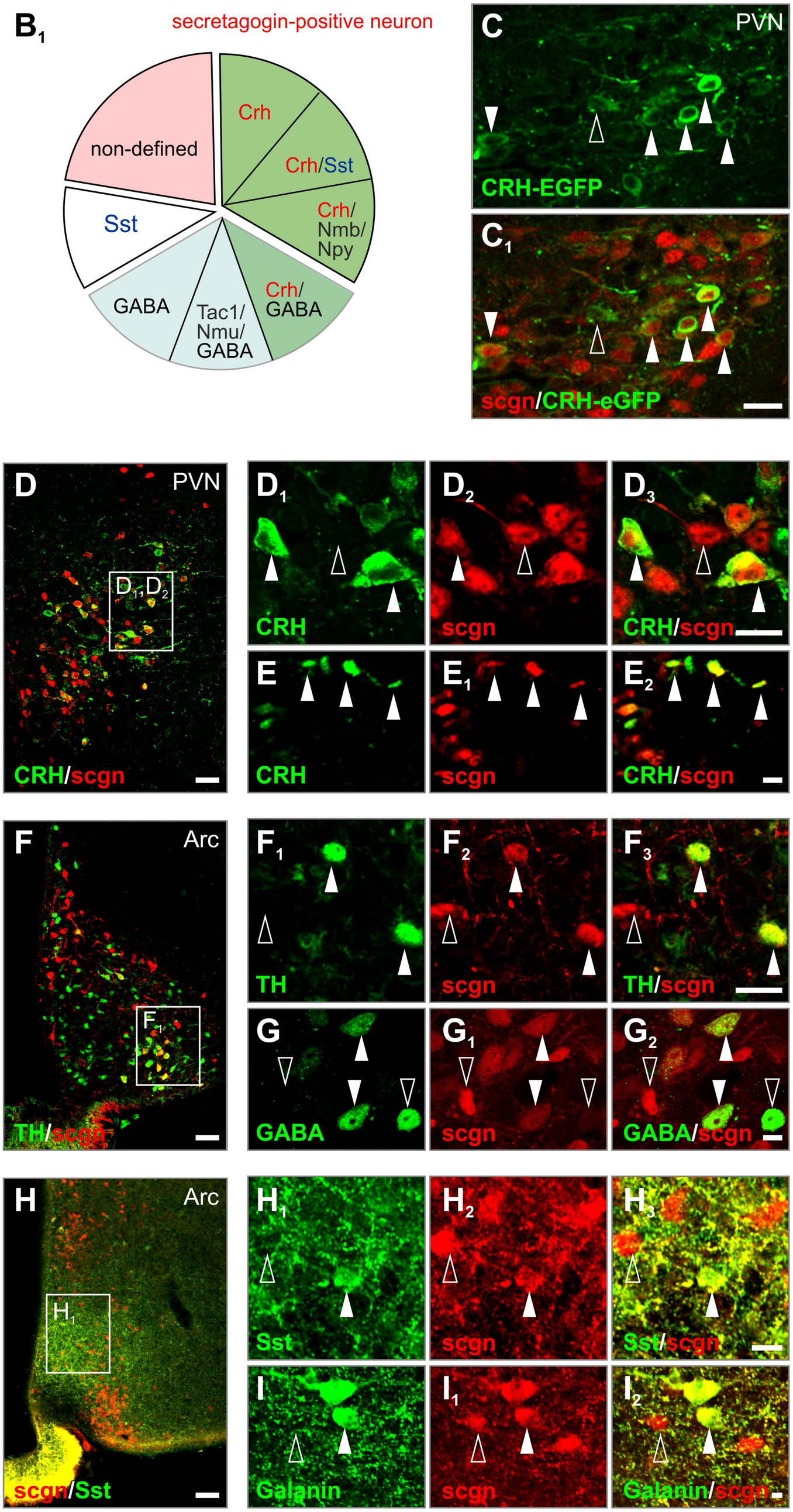
B1
secretagogin-positive neuron
non-defined
Crh
Crh/Sst
Crh/ Nmb/ Npy
Sst
GABA
Tac1/ Nmu/ GABA
Crh/ GABA
C
PVN
CRH-EGFP
C1
scgn/CRH-eGFP
D
PVN
D1, D2
CRH/scgn
D1
CRH
D2
scgn
D3
CRH/scgn
E
CRH
E1
scgn
E2
CRH/scgn
F
Arc
F1
TH/scgn
F1
TH
F2
scgn
F3
TH/scgn
G
GABA
G1
scgn
G2
GABA/scgn
H
Arc
H1
scgn/Sst
H1
Sst
H2
scgn
H3
Sst/scgn
I
Galanin
I1
scgn
I2
Galanin/scgn

Romanov, Alpar *et al*. - Figure 5R1 EMBOJ-2014-88977 (1.5 columns)

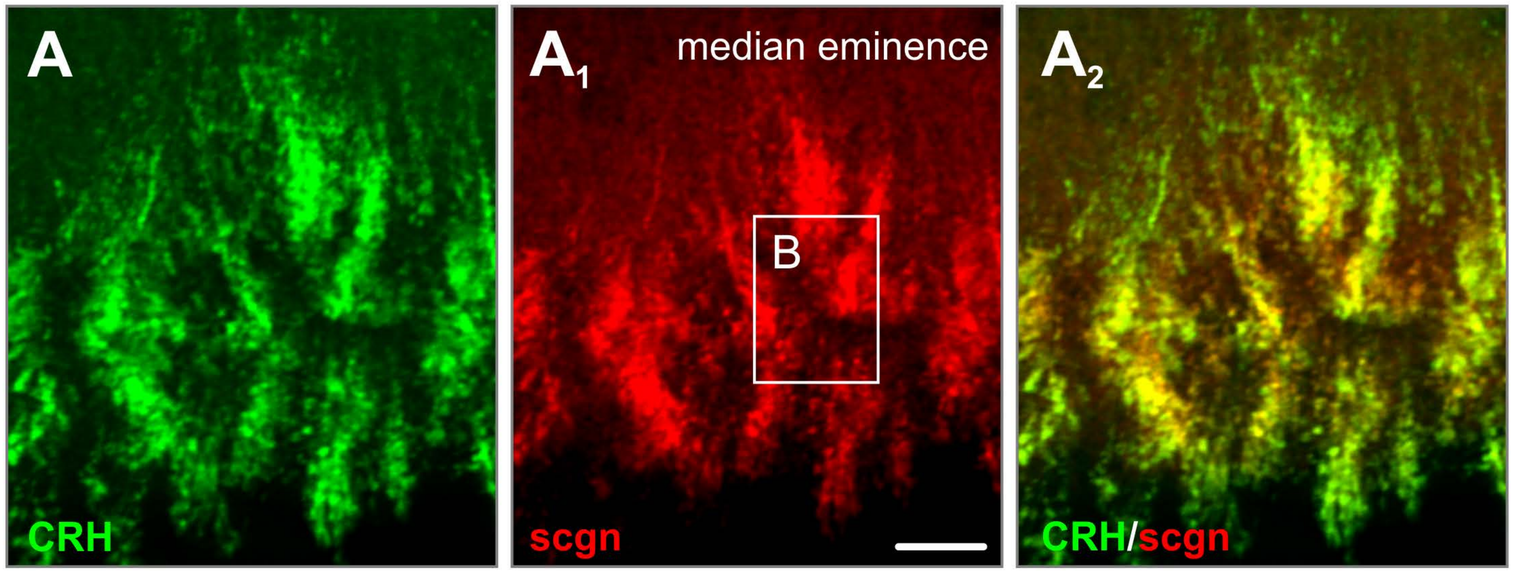

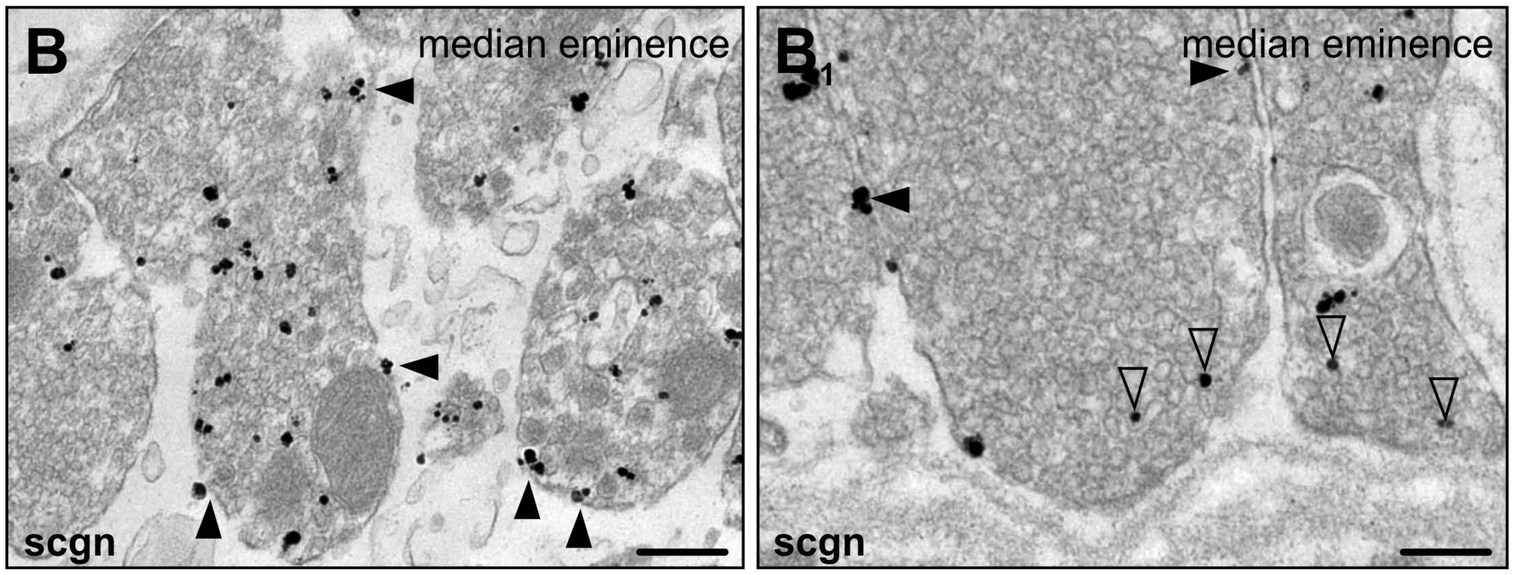

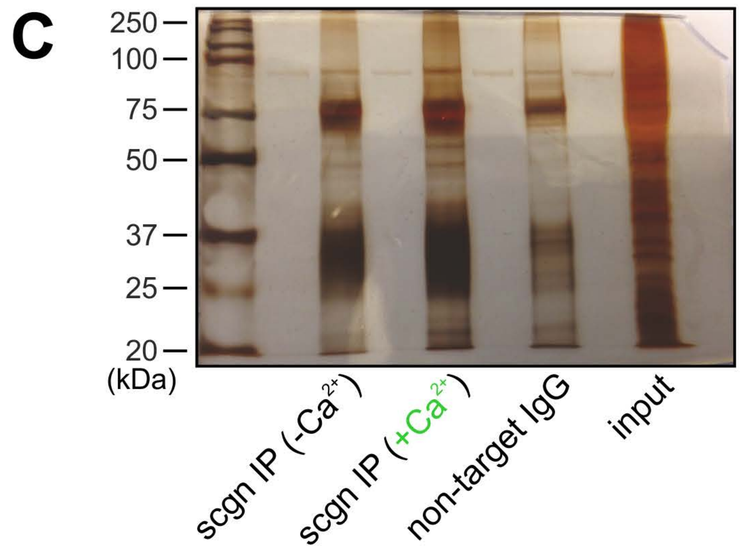

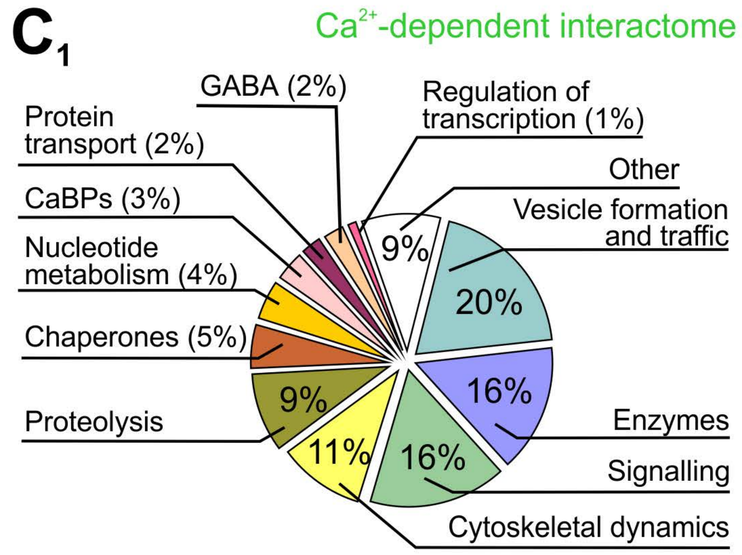

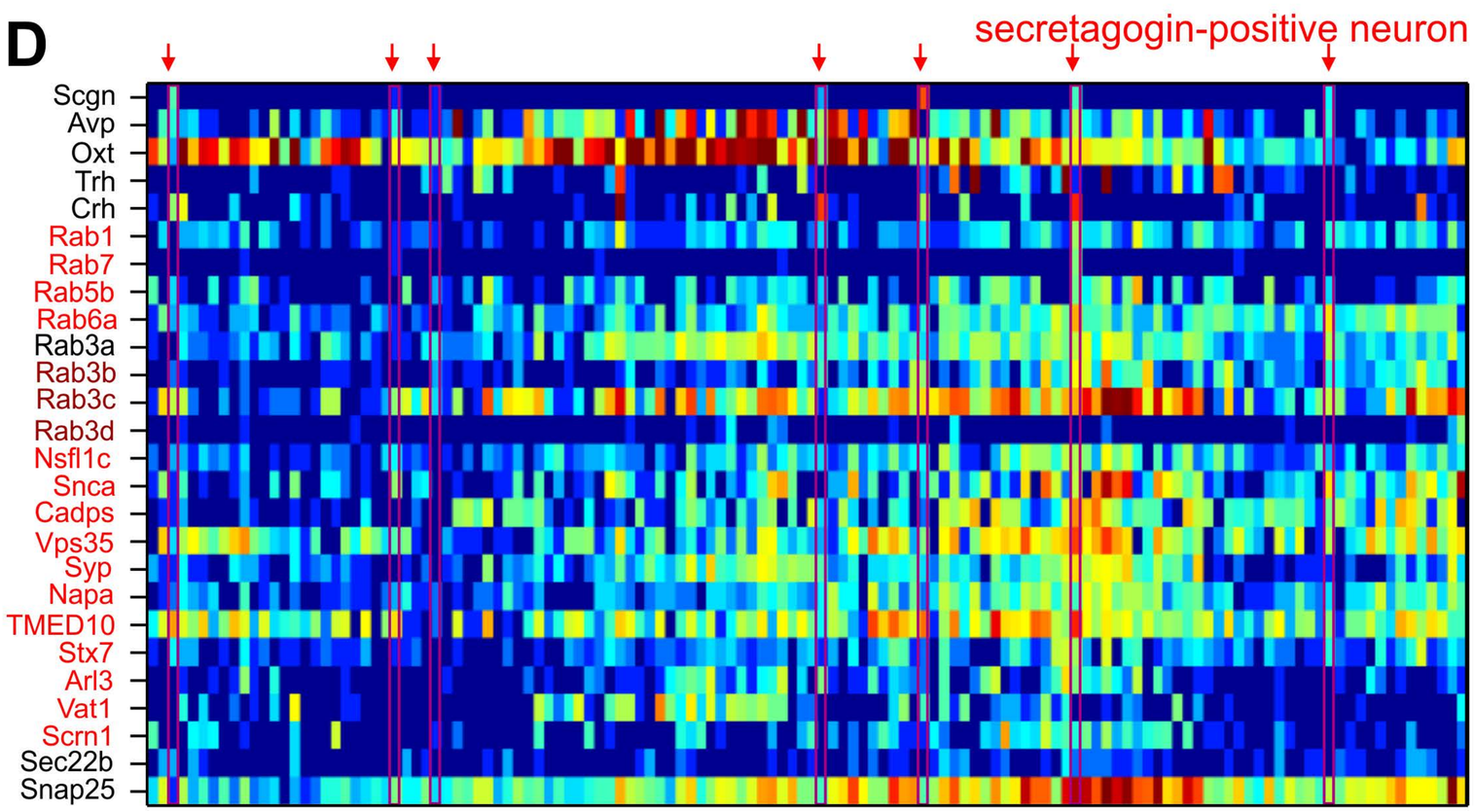

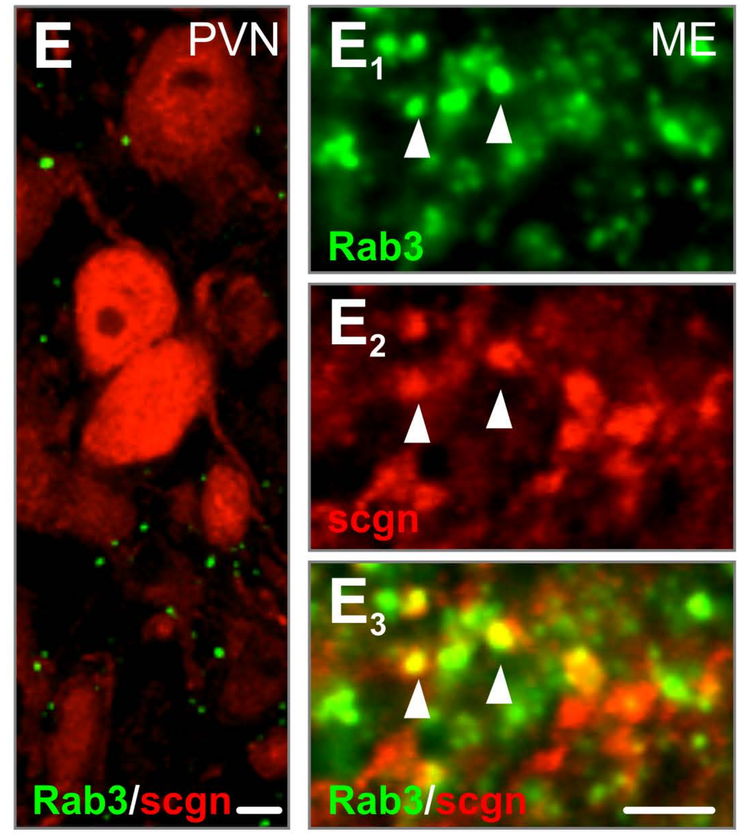

Romanov, Alpar *et al*. - Figure 6R1
EMBOJ-2014-88977 (single column)

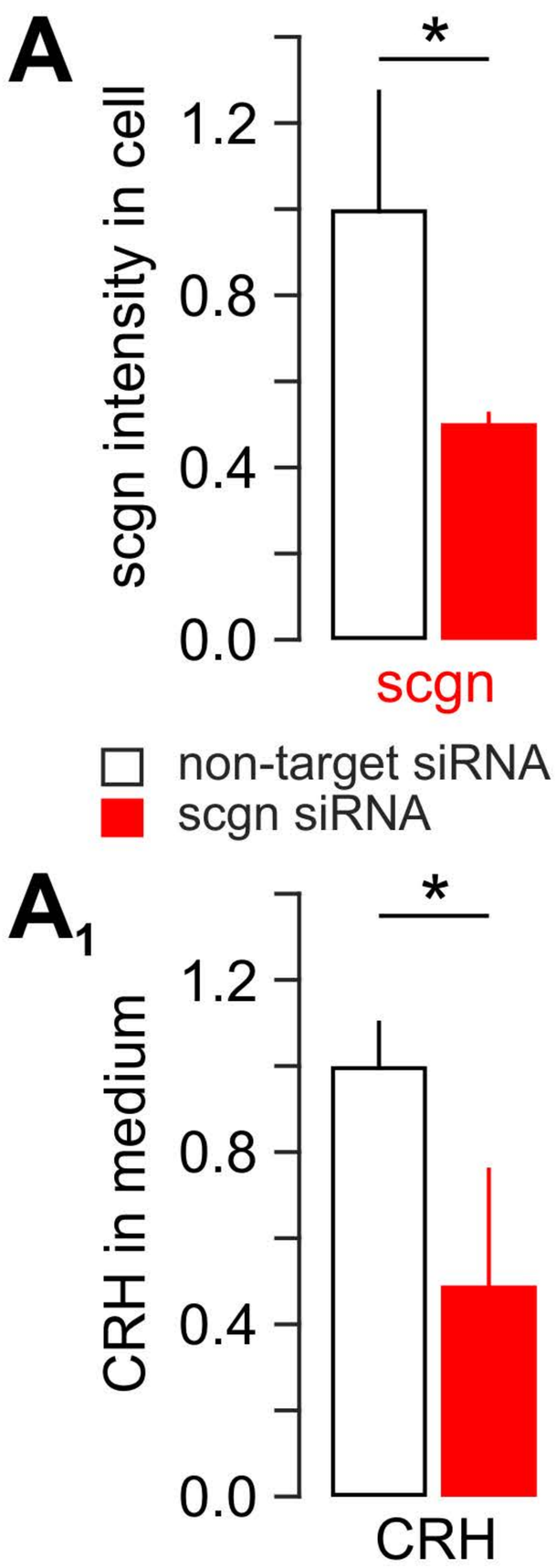

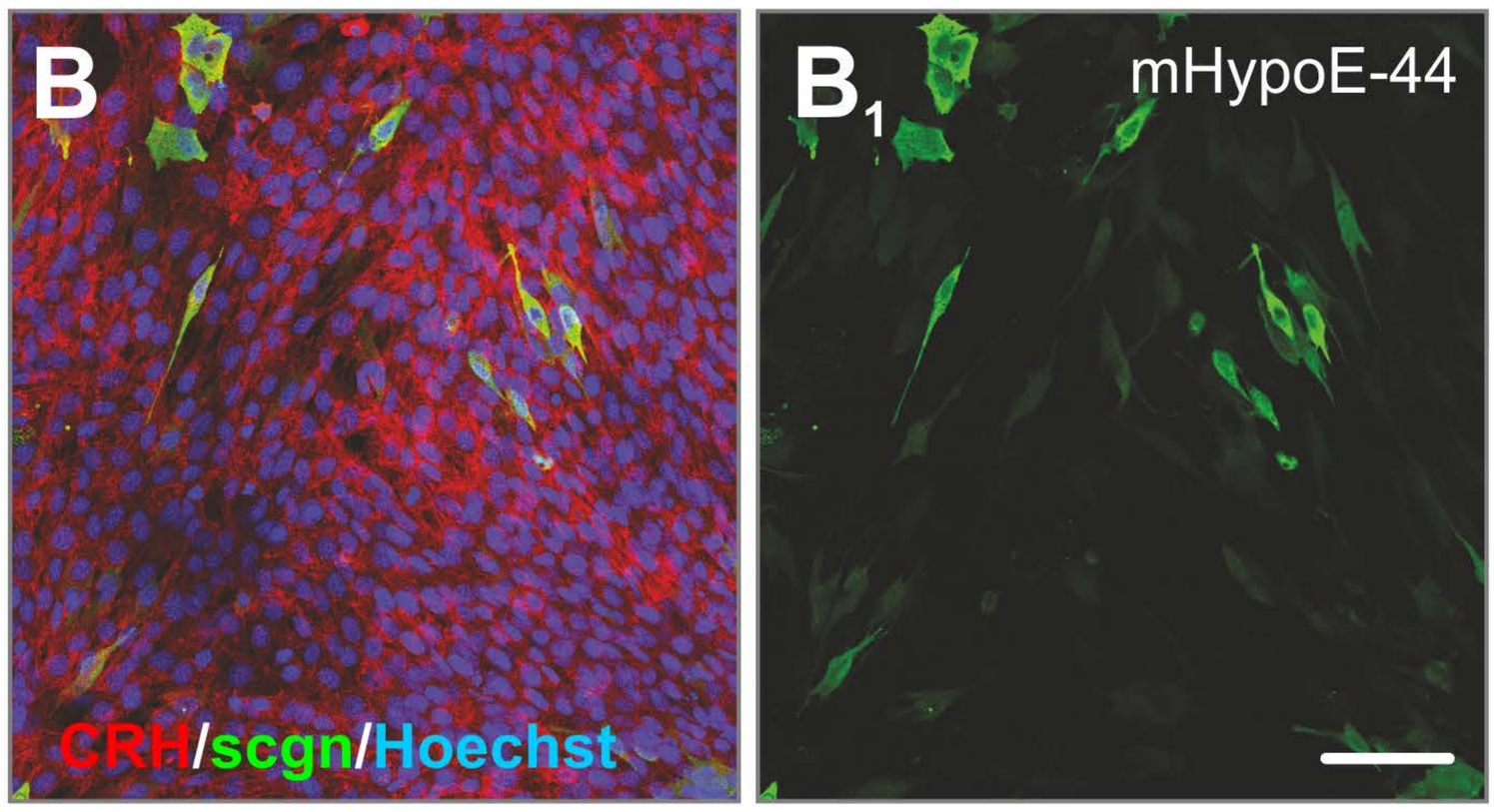

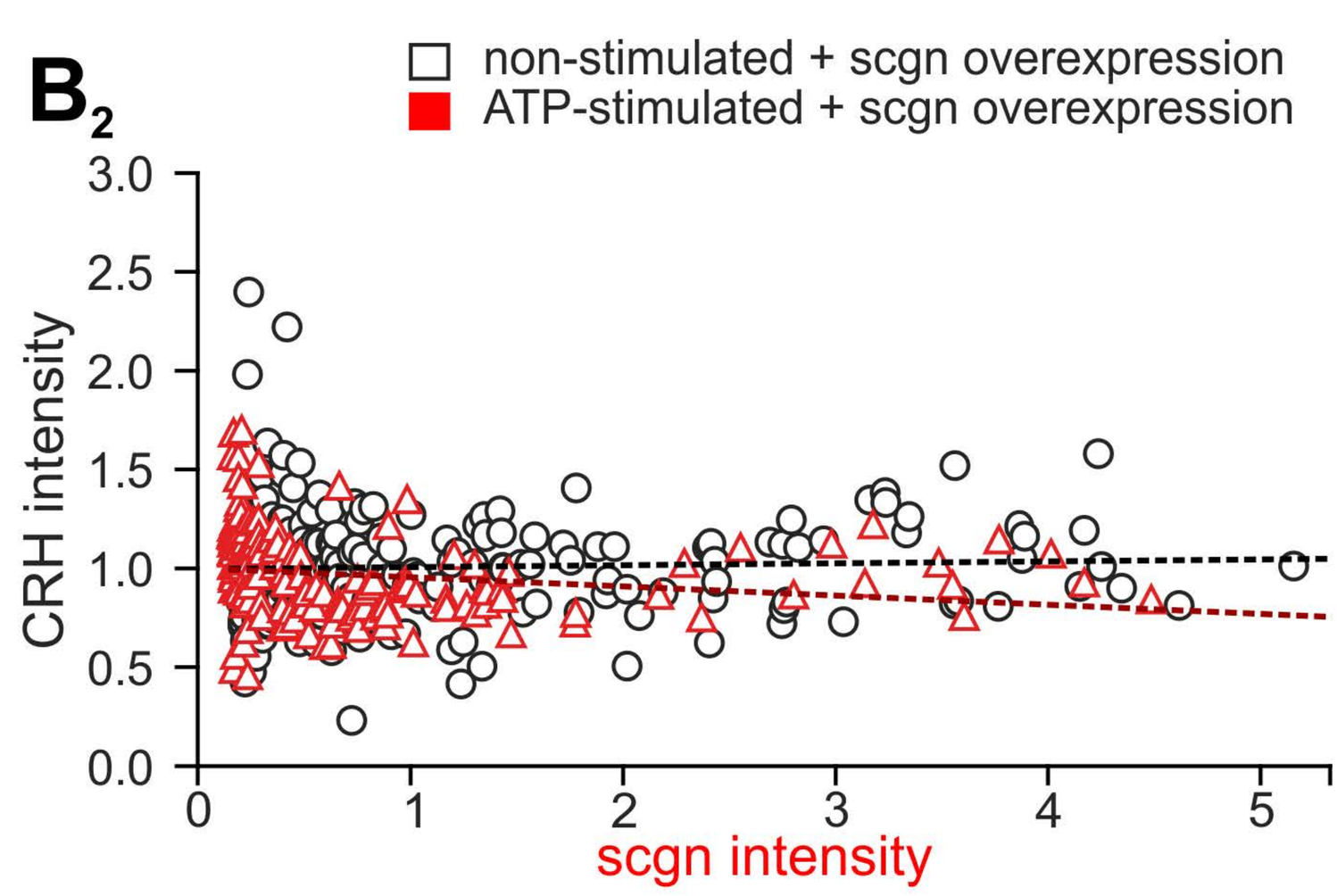

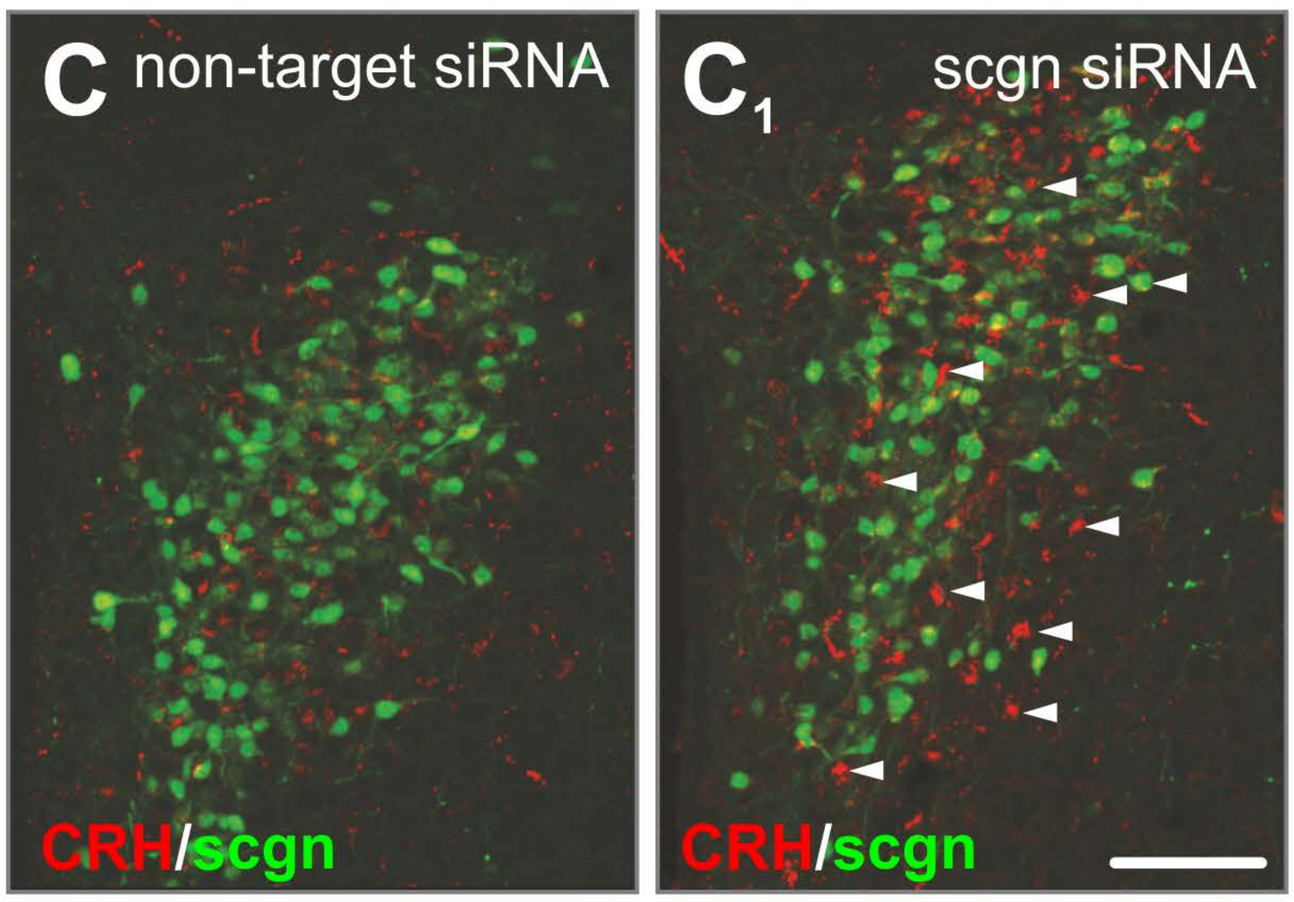

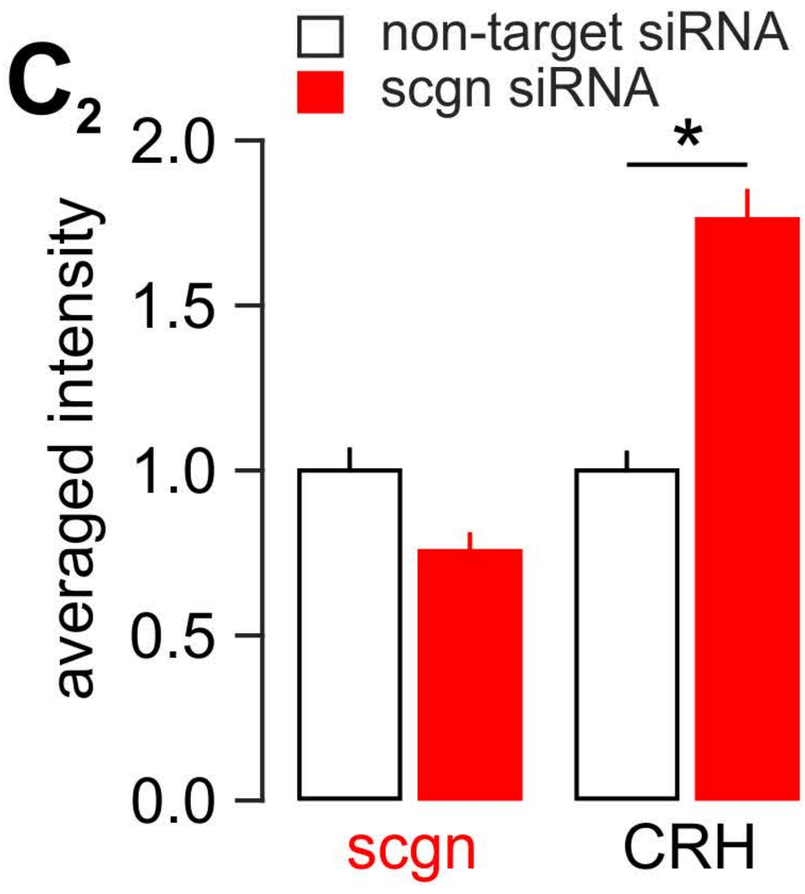

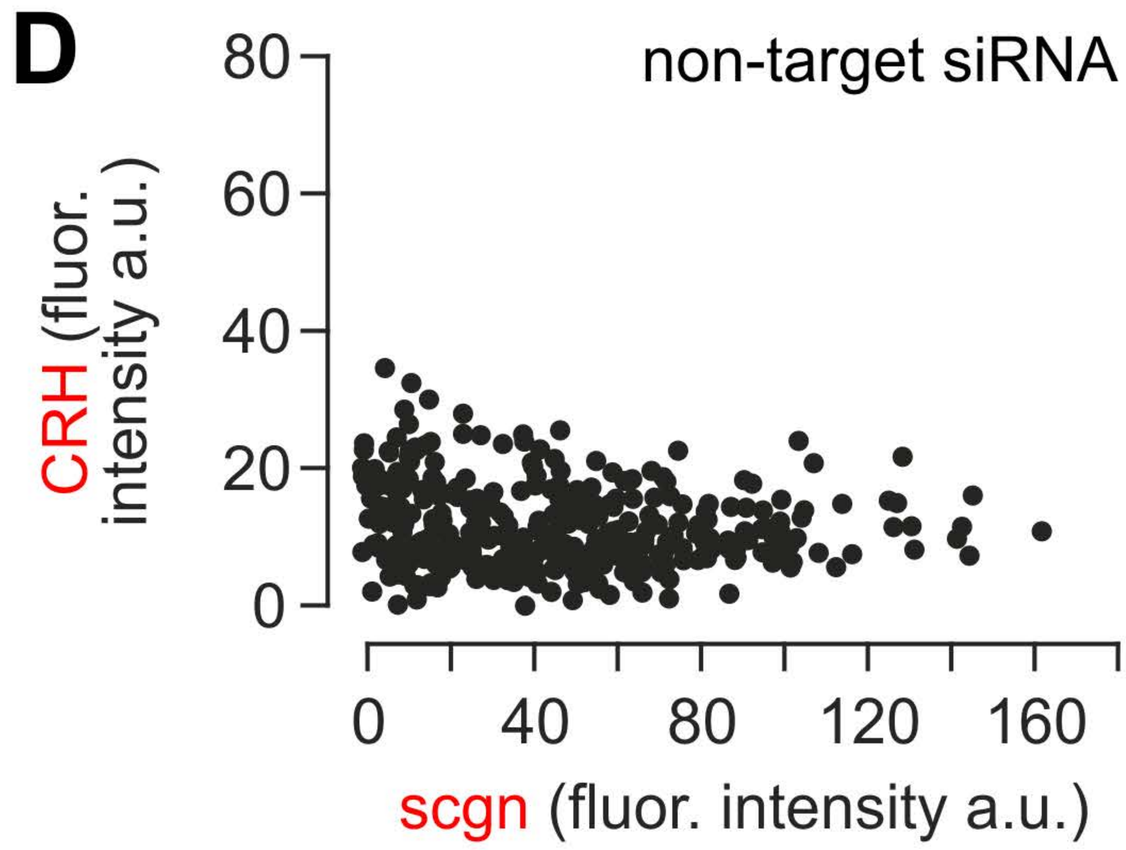

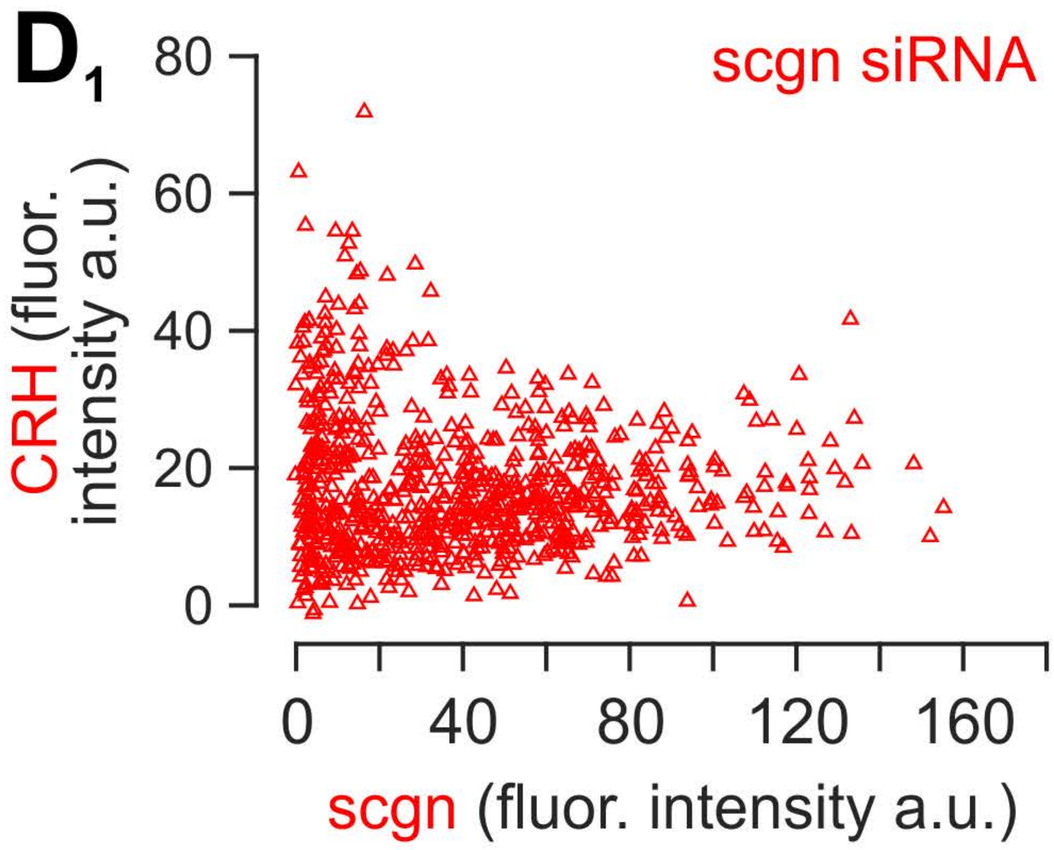

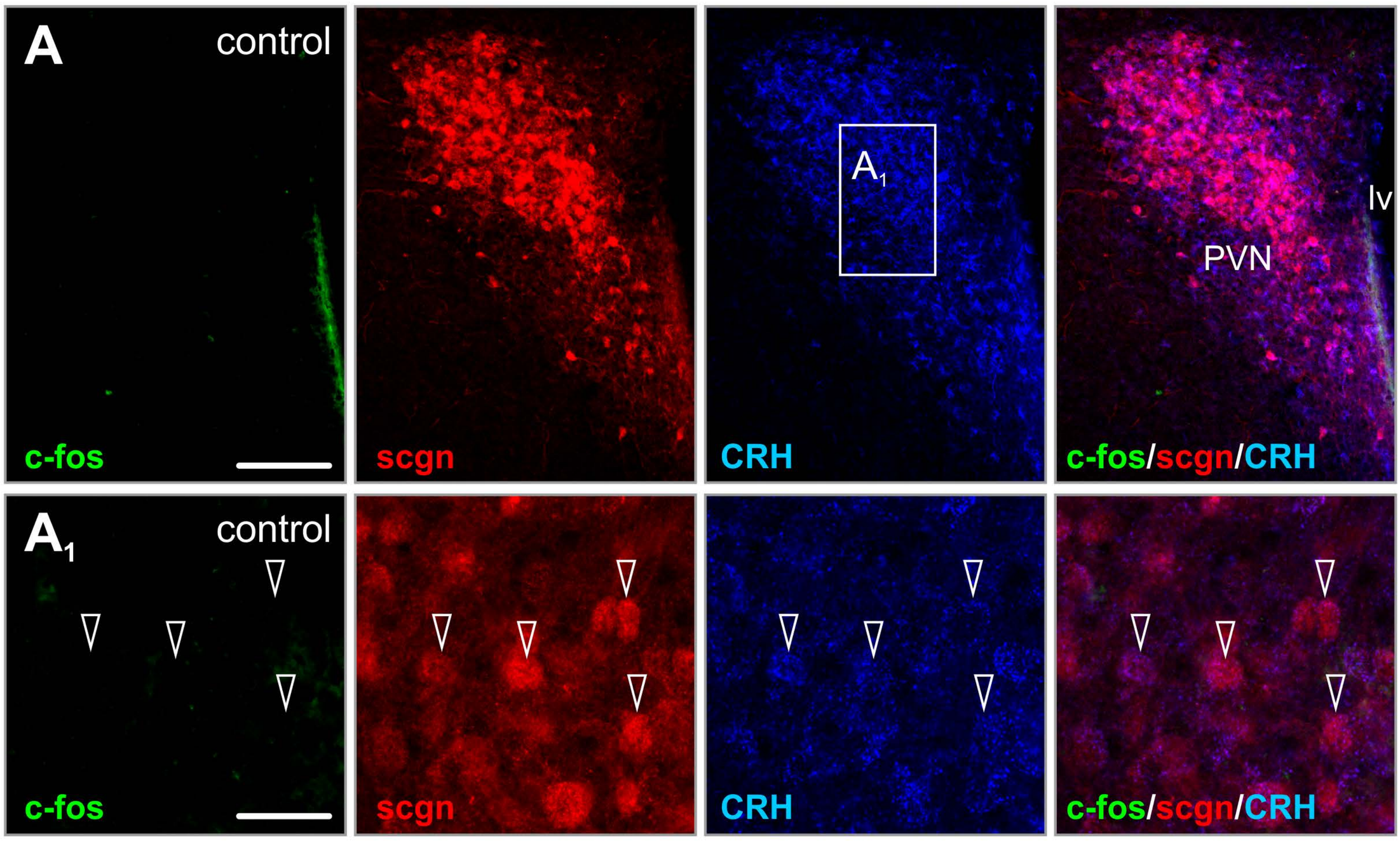
A
control
c-fos
scgn
CRH
A1
PVN
lv
c-fos/scgn/CRH
A1
control
c-fos
scgn
CRH
c-fos/scgn/CRH
B
6h post-stress
c-fos
scgn
CRH
B1
PVN
lv
c-fos/scgn/CRH
B1
6h post-stress
c-fos
scgn
CRH
c-fos/scgn/CRH

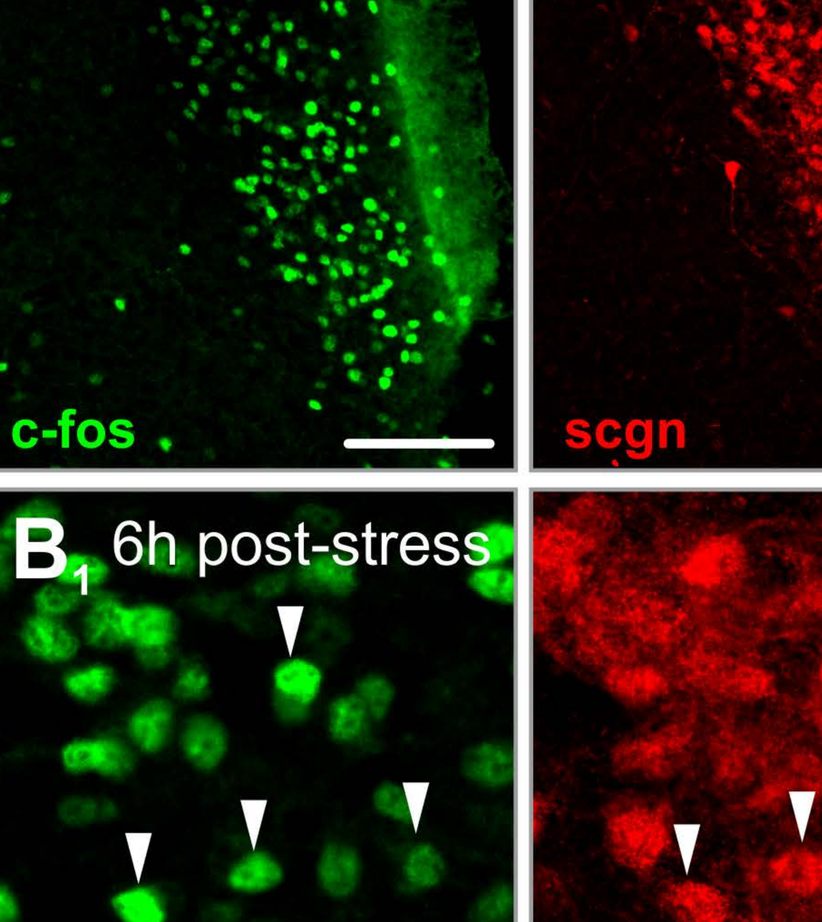
C
ACTH (fmol/ml serum)
300
200
100
0
*
control
formalin-
stressed

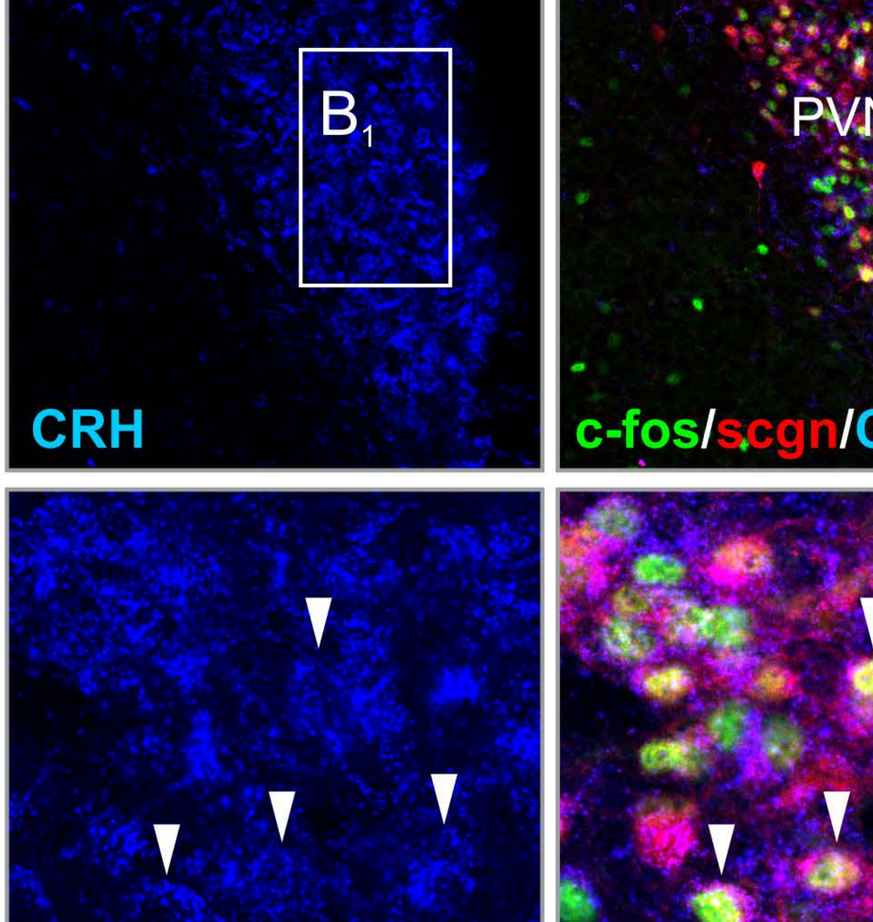
D
corticosteron
(nmol/ml serum)
2.0
1.5
1.0
0.5
0
*
control
formalin-
stressed